Journal Pre-proof


# HSPB6: A lipid-dependent molecular chaperone inhibits α-synuclein aggregation

Valentina Secco, Tatiana Tiago, Roxine Staats, Swapan Preet, Sean Chia, Michele Vendruscolo, Serena Carra

PII: S2589-0042(24)01882-0

DOI: https://doi.org/10.1016/j.isci.2024.110657

Reference: ISCI 110657

To appear in: *ISCIENCE*

Received Date: 3 May 2024

Revised Date: 9 June 2024

Accepted Date: 31 July 2024

Please cite this article as: Secco, V., Tiago, T., Staats, R., Preet, S., Chia, S., Vendruscolo, M., Carra, S., HSPB6: A lipid-dependent molecular chaperone inhibits α-synuclein aggregation, *ISCIENCE* (2024), doi: https://doi.org/10.1016/j.isci.2024.110657.

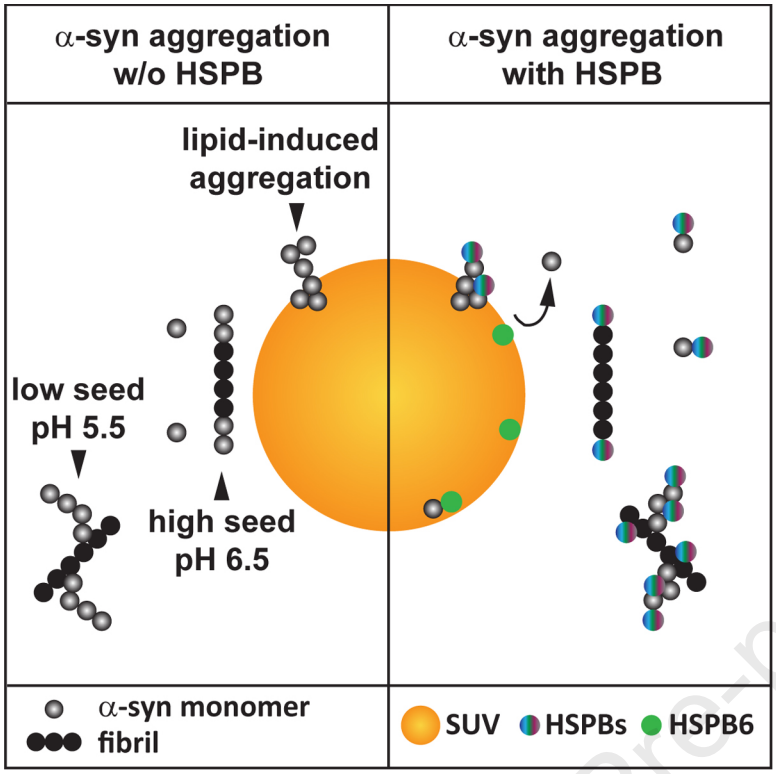

# HSPB6: A lipid-dependent molecular chaperone inhibits α-synuclein aggregation

**Authors**

Valentina Secco[1,†], Tatiana Tiago[1,†], Roxine Staats[2], Swapan Preet[2], Sean Chia[2], Michele Vendruscolo[2,*], Serena Carra[1,3,*]

**Affiliations**

[1]*Department of Biomedical, Metabolic and Neural Sciences, University of Modena and Reggio Emilia, Modena, Italy*

[2]*Centre for Misfolding Diseases, Yusuf Hamied Department of Chemistry, University of Cambridge, Cambridge, UK*

[3]*Lead contact*

† "These authors contributed equally to this work"

* Corresponding authors: Michele Vendruscolo, mv245@cam.ac.uk; Serena Carra, serena.carra@unimore.it



**Summary**

The process of protein misfolding and aggregation is associated with various cytotoxic effects. Understanding how this phenomenon is regulated by the protein homeostasis system, however, is difficult, since it takes place through a complex non-linear network of coupled microscopic steps, including primary nucleation, fibril elongation and secondary nucleation, which depend on environmental factors. To address this problem, we studied how the aggregation of α-synuclein, a protein associated with Parkinson's disease, is modulated by molecular chaperones and lipid membranes. We focused on small heat shock proteins (sHSPs/HSPBs), which interact with proteins and lipids and are upregulated during aging, a major risk factor for protein misfolding diseases. HSPBs act on different microscopic steps to prevent α-synuclein aggregation, with HSPB6 showing a lipid-dependent chaperone activity. Our findings provide an example of how HSPBs diversified their mechanisms of action to reach an efficient regulation of protein misfolding and aggregation within the complex cellular environment.

**Introduction**

α-Synuclein (α-syn) is an intrinsically disordered protein with an N-terminal domain (residues 1–60) that adopts an α-helical conformation upon binding to phospholipid membranes, a central hydrophobic non-β-amyloid component (NAC) domain (residues 61–95) that adopts β-sheet structures upon aggregation, and a negatively charged C-terminal domain (residues 96-140) that can bind to calcium ions[1]. α-syn is highly expressed in the brain, where it is associated with synaptic vesicles and regulates synaptic transmission[2,3]. α-syn preferentially binds to lipid membranes and regulates different aspects of vesicular dynamics, from vesicle tethering to fusion and exocytosis[4].

Like other intrinsically disordered peripheral membrane proteins, α-syn exists in a soluble and membrane-bound form. Unbound α-syn and monomeric α-syn adopt partially folded intermediate conformations; upon binding to lipid membranes, α-syn adopts an α-helical structure[5]. However, binding to lipids represents a double-edged sword, because it can promote α-syn oligomerization and amyloid formation, which contribute to the development of a group of neurodegenerative disorders called synucleinopathies[6-8]. Synucleinopathies include Parkinson's disease (PD), dementia with Lewy bodies (DLB), and multiple-system atrophy (MSA). PD is characterized by intracellular deposits called Lewy bodies (LBs)[9], which are heterogenous in composition and contain amyloid fibrils of α-syn, but also other proteins such as molecular chaperones and large amounts of lipids and membranous organelles [10]. Of note, several disease-linked mutations are found in the α-syn N-terminal membrane-binding region and affect α-syn association with lipid droplets and vesicles, promoting its aggregation[11]. Moreover, lipid alterations have been identified in the brain and plasma of patients affected by PD, and mutations in the glucosylceramidase-beta (GBA) gene, which affect the sphingolipid metabolism, are an important risk factor in PD and DLB[12]. Additional genes involved in glycerophospholipid and sphingolipid metabolism, namely the PLA2G6 and SCARB2 genes, are also considered risk factors for PD[13]. Taken together, these findings support a lipid-centric view of α-syn aggregation and suggest that identifying approaches that limit α-syn lipid-induced aggregation may open new therapeutic avenues[14].

α-syn aggregation is a multi-step process that involves several interconvertible conformational states, transient oligomeric states and prefibrillar species, which are influenced by environmental factors such as lipids and pH[15]. The main steps that can be identified for α-syn aggregation: (i) primary nucleation, in which monomers assemble to form disordered oligomeric species; oligomer conversion, in which these oligomeric species convert into ordered fibrillar seeds rich in β-structures; (ii) elongation, in which the seeds grow to generate protofibrils and fibrils; and (iii) secondary nucleation, a step in which monomers assemble on the surface of fibrils to generate new fibrils and new oligomeric species[15]. An additional pathway that can promote α-syn aggregation has been recently identified: liquid-liquid phase separation of α-syn into condensates that can mature into amyloid hydrogels containing α-syn oligomers and fibrillar species[16-18]. Of note, because of the high concentration within condensates, α-syn primary nucleation can be readily observable at physiological pH, which is followed by the rapid growth and amplification of α-syn aggregates[19].

Molecular chaperones, mainly heat shock proteins (HSPs), combat protein aggregation, delaying the growth of amyloid fibrils[20] and preventing the conversion of liquid-like condensates into amyloid hydrogels[21]. For example, the ATP-dependent chaperone HSP70, a master regulator of protein homeostasis (proteostasis), interacts with α-syn monomers, oligomers and prefibrillar species, protecting against α-syn-mediated toxicity in cellular and animal models of PD[22]. In addition, a molecular chaperone complex containing Hsc70 and the co-chaperone Hsp40/DnaJB1 and Apg2 can remove α-syn monomers from the fibril ends, reverting the aggregation process[23]. Also the small HSPs/HSPBs, which are ATP-independent chaperones and include 10 members in humans (HSPB1-HSPB10)[24], can prevent α-syn aggregation. For example, HSPB1 (Hsp27), HSPB2 (MKBP), HSPB3 (HSPL27), HSPB5 (αB-crystallin) and HSPB8 (Hsp22) bind to α-syn fibrils and inhibit fibril elongation and maturation[25-30]. In addition, HSPBs colocalize with LBs, and their expression levels are upregulated in brain regions characterized by

neurodegeneration in protein misfolding diseases such as PD[31,32]. Together these observations support the view that molecular chaperones, including HSPBs, play an active role in preventing α-syn aggregation. Yet these studies have focused on a protein-centric view of α-syn aggregation and the mode of action of molecular chaperones. However, molecular chaperones can bind to lipids[33-35] and α-syn association with lipids enhances the rate of aggregation[7,36]. We still poorly understand the mechanisms regulating the binding of molecular chaperones to lipids and their functional roles. The association of HSPs with lipids has been suggested to stabilize membranes upon stress conditions, including heat shock, to regulate endo-lysosomal trafficking, endocytosis and cancer cell invasion, with important physiological and pathological implications[35,37-39]. A number of proteins, including the fatty acid-binding proteins (FABPs), have been proposed to act as "lipid chaperones", a term that refers to molecular chaperones that have lipids, rather than proteins, as substrates[40]. In addition, the "lipid-chaperone hypothesis" states that free lipid molecules can interact with proteins forming water-soluble lipid−protein complexes that promote protein anchoring to the membranes, influencing their stability[41]. Yet, whether or not the anti-aggregation activity of molecular chaperones depends on specific types of lipid membranes remains unknown. Here we addressed this question focusing on HSPBs and α-syn as a model protein.

HSPBs are characterized by a low molecular weight (12-43 kDa) and the presence of a highly-conserved α-crystallin domain of 80-100 amino acids, flanked by less conserved N-terminal and C-terminal intrinsically disordered domains[42]. All these regions are involved in regulating the assembly of HSPB monomers into polydisperse oligomers that are thought to act as a cellular chaperone reservoir[43]. Human HSPBs show a high structural diversity and can assemble into dynamic oligomers of different size and compositions. HSPB1, HSPB4, and HSPB5 co-assemble into polydisperse oligomers, while HSPB6, HSPB7 and HSPB8 mainly exist in form of dimers[44,45] and HSPB3 can form tetramers with HSPB2 at a 1:3 ratio[46]. Upon stress conditions such as changes in the temperature, pH and ion concentrations and in presence of unfolded and misfolded proteins, HSPB assemblies dissociate into smaller oligomers, dimers and monomers giving rise to an HSPB ensemble with chaperone activity that can bind to and neutralize non-native and aggregation-prone intermediates, preventing their irreversible aggregation[42]. Recent studies that analyzed the accessible surface areas of small HSPs of different origins showed that upon dissociation of the larger oligomers, the α -crystallin domain of the resultant monomers and dimers are partially unfolded and display enhanced chaperone activity[47]. Thus, the dynamic release of disordered monomers/dimers has been proposed to represent a common mechanism of action for small HSPs[47]. Nevertheless, due to the ability of HSPBs to interact with each other to form homo- and hetero-oligomers of variable size, which influences their affinity for different substrates, one would not expect their chaperone activity to be described with one unifying mechanism. Rather, distinct mechanisms may exist dependent on the type of HSPB, the type of substrate and the surrounding environment, such as pH, salinity and presence of lipids[48].

Using a three-pronged kinetic approach previously developed[7,11], we tested here the ability of selected HSPBs to inhibit α-syn lipid-induced aggregation, as well as fibril growth in absence of lipids. The chaperone activity of HSPB1, HSPB4 and HSPB5 on α-synuclein has been characterized in detail by previous groups[25-29,49-54]. Here we focused on the less-well studied HSPB members that tend to mainly form dimers/small oligomers. Since both HSPB1 and HSPB5 typically form large oligomers and were both previously shown to bind to lipids[35], we selected HSPB5 for comparative analysis, while focusing on the other less characterized members of the family that mainly form dimers/smaller oligomers. Our findings identify HSPB6 as a lipid-dependent molecular chaperone, since it could efficiently prevent α-syn aggregation only in presence of lipid membranes. Instead, the other HSPBs tested showed stronger chaperone activity in presence of monomeric α-syn and preformed α-syn fibrils, and a moderate chaperone activity in presence of lipid membranes. These results highlight the diversity and complexity of HSPBs, which diversified their mechanisms of action to reach an efficient regulation of protein aggregation within the complex lipid-enriched cellular environment. We anticipate that the classification of poor and efficient chaperones based on protein-only assays will warrant further investigation, and the identification of other lipid-

dependent molecular chaperones similar to HSPB6 may represent the first step towards new potential therapeutic avenues.

**Results**

**HSPBs inhibit α-syn lipid-induced aggregation**

A three-pronged approach is proposed to dissect the key steps of α-syn aggregation, namely lipid-induced aggregation, elongation and secondary nucleation (Fig. 1). The assay to monitor α-syn aggregation induced by lipids has been developed to study α-syn aggregation at physiological concentrations, which are estimated to be lower than 30 - 60 μM and in presence of small unilamellar vesicles (SUVs), which trigger α-syn amyloid fibril formation (Fig. 1, left panel)[7,11,55]. Primary nucleation is followed by fibril growth by elongation, which can be studied using a second assay (in absence of lipids) through addition of monomeric α-syn to the growing extremity of existing fibrils at high concentration (Fig. 1, middle panel, high-seed). Finally, secondary nucleation events that occur via formation of surface-catalysed aggregates and lead to fibril amplification are monitored under conditions of mildly acidic pH and low fibril concentration (Fig. 1, right panel, low seed)[11,56]. These mildly acidic environmental conditions mimic the low pH (5.5) that characterizes dopaminergic neurons, which express highest levels of α-syn [57]. Using this three-pronged approach we evaluated the impact of individual HSPBs on α-syn aggregation, identifying the contribution of specific environmental factors that are biologically relevant such as lipid composition and pH variation.

In these assays, α-syn amyloid fibril formation is followed over time by measuring the increase of Thioflavin T (ThT) fluorescence. We previously reported that the kinetics of α-syn aggregation are accelerated upon incubation of α-syn monomers with SUVs prepared from the model membrane lipid DMPS (1,2-dimyristoyl-sn-glycero-3-phospho-L-serin)[6,7,58] (Fig. 1, left panel and Fig. 2, black curves). Although of limited physiological relevance, DMPS SUVs represent a well-established model to study α-syn lipid-induced aggregation and were used as the reference system here. The diameter of DPMS lipid vesicles was measured prior to their use for each experiment; a representative measure of DMPS lipid in shown in Supplementary Fig. 1A. No increase in the ThT fluorescence signal was detected in absence of DMPS under the experimental conditions used, while α-syn amyloid fibril formation started already after 5 h of co-incubation with DMPS SUVs and reached a plateau after circa 25 h (Fig. 2A, black curve), when the molecules of monomeric α-syn, initially present in the reaction mixture, were incorporated into the growing fibril. Thus, the lower the time required to reach the plateau and the steeper the curve slope, the higher the rate of α-syn aggregation. We then co-incubated DMPS with α-syn and either HSPB3, HSPB5, HSPB6, HSPB7 or HSPB8 starting with an HSPB:α-syn ratio of 1:100. HSPB6 completely inhibited α-syn lipid-induced aggregation on the timescale that we monitored (100 h) (Fig. 2A). Instead, HSPB3, HSPB5, HSPB7 and HSPB8 delayed α-syn lipid-induced aggregation at low stoichiometries, but with different degrees of efficacy, with HSPB3 showing the poorest chaperone activity (Fig. 2A, B). The beginning of the aggregation occurred circa 5 h after coincubation of DMPS with α-syn alone (Fig. 2A, black curve) and was delayed to about 25 - 35 - 40 and 45 h in presence of HSPB3, HSPB7, HSPB8 and HSPB5, respectively, while it never occurred with HSPB6 (Fig. 2A, colored curves). The rate at which the α-syn fibrils grow is indicated by the slope of the curve. By comparing the slope of the curves in absence or presence of HSPB3, HSPB5, HSPB7 and HSPB8 we deduced that the aggregation process proceeded with similar kinetics to the control condition (α-syn) (Fig. 2A). Thus, at the HSPB:α-syn ratio of 1:100 only HSPB6 completely abrogated α-syn lipid-induced aggregation.

We next applied a previously proposed lipid-induced aggregation model [7] to our data to compare the efficacy of the HSPBs studied. In this model, the nucleation process is assumed to occur at the surface of the vesicles and then to be followed by the growth of fibrils from lipid-bound α-syn. We calculated the half time (t1/2) of α-syn aggregation alone or in presence of HSPBs. At the HSPB:α-syn ratio of 1:100, HSPB3 had the lowest efficacy, with an aggregation half time of ca. 30 hours (Fig. 2B). HSPB6 was excluded from this analysis since it completely

abrogated α-syn lipid-induced aggregation at the HSPB:α-syn ratio of 1:100 (Fig. 2B). The same experiments were then conducted at higher stoichiometries using, respectively, the HSPB:α-syn ratio of 1:200 (Fig. 2C, D) and 1:400 (Fig. 2E, F). At the lowest HSPB:α-syn ratio of 1:50, all the HSPB tested could prevent α-syn lipid-induced aggregation (Fig. 2G). HSPB efficacy was further compared by measuring the relative aggregation constant normalized for the aggregation rate, using a previously published one-step nucleation model.[7] Using this model, we confirmed that HSPB3 had the lowest efficacy, with a relative aggregation rate ratio to α-syn alone of 0.10 (Supplementary Fig. 1B); instead, HSPB5, HSPB7 and HSPB8 reduced the lipid-induced aggregation with a relative aggregation rate ratio between 0.05 and 0.07 (Supplementary Fig. 1B). HSPB6 was excluded from this analysis since it completely inhibited α-syn lipid-induced primary-nucleation at the 1:100 HSPB:α-syn ratio. When using higher HSPB:α-syn ratios, we confirmed the strongest inhibitory effect of HSPB6 in presence of lipids compared to the other HSPBs tested (Supplementary Fig. 1C and D). Thus, although all HSPBs prevented α-syn lipid-induced aggregation in a dose-dependent manner, HSPB6 showed the greatest efficacy.

Considering that previous reports showed that HSPB5 and HSPB8 interact both with α-syn and lipids[26,28,33,35,54], these results are compatible with at least two possible, but not mutually exclusive, incompatible, mechanisms: HSPBs compete with α-syn for binding to lipid membranes, thus reducing α-syn lipid-induced aggregation; HSPBs bind to α-syn monomers, thus preventing their binding to the lipid surface. Alternatively, HSPBs bind to α-syn embedded in the lipids, shielding it from oligomerization and aggregation. To differentiate between these possible mechanisms, we next tested whether HSPB3, HSPB5, HSPB6, HSPB7 or HSPB8 can interact with lipid membranes.

Proteins embedding into lipid membranes affect their fluidity and melting temperature, which can be measured by monitoring changes in the polarisation of the fluorescence of the probe diphenylhexatriene (DPH): the higher the anisotropy of DPH, the lower the membrane fluidity[59]. We previously showed that DMPS SUVs convert at 41 ˚C from a gel phase bilayer with solid hydrocarbon chain into a liquid crystalline bilayer with fluid hydrocarbon chain[6]. In presence of α-syn, the melting temperature of DMPS SUVs bound to α-syn decreases and is centered at 25 ˚C[6]. Since temperature fluctuations affect lipid phase transitions, which can in turn modify the binding affinity of proteins for lipids, we measured how the microviscosity of DMPS SUVs changes in absence or presence of HSPBs by monitoring the DPH fluorescence polarisation at increasing temperature (Supplementary Fig. 2A, brown dotted line). The impact of the various HSPBs on DHP fluorescence polarization was compared to that of α-syn, employed as a positive control, in the temperature range from 25 to 50 °C[6,7] (Supplementary Fig. 2A, compare the brown dotted line with the black line). As expected[6], coincubation of DPMS with α-syn decreased the DPH fluorescence polarization in the temperature range investigated (Supplementary Fig. 2A). HSPB3, HSPB5 and HSPB7 increased the DHP fluorescence polarization when co-incubated at temperatures ranging from circa 25 – 37 °C, whereas at higher temperatures they decreased the DHP fluorescence polarization, except for HSPB7 (Supplementary Fig. 2A). HSPB8 and HSPB6 decreased the DPH fluorescence polarization from and above circa 30 °C, with a stronger impact of HSPB6 compared to HSPB8 (Supplementary Fig. 2A). These data suggest that all HSPBs tested can influence the dynamical and structural properties of lipid bilayers measured via DHP fluorescence polarization at different temperatures.

We next tested whether HSPBs can influence the DPH fluorescence polarization upon co-incubation with DMPS and α-syn, starting with a HSPB:α-syn ratio of 1:1 (Supplementary Fig. 2B). Compared to α-syn alone (Supplementary Fig. 2B, black line), HSPB6 further decreased the DPH fluorescence polarization at the physiological temperature (37 °C) and above; HSPB3, HSPB5 and HSPB7 increased the DPH fluorescence polarization in the temperature range from circa 37 - 50 °C), while HSPB8 had no effect (Supplementary Fig. 2B, compare grey line with black line). Since higher DPH anisotropy is indicative of lower membrane fluidity, we conclude that, compared to DMPS SUVs incubated with α-syn alone, in the temperature range from circa 35 – 50 °C, HSPB3, HSPB5 and HSPB7 tend to restore membrane fluidity, whereas HSPB6 further decreased it, showing an additive effect with α-syn, and HSPB8 had no impact. The additive effect of HSPB6, compared to DMPS and

α-syn alone, was further confirmed by lowering the concentration of HSPB6 by four times (HSPB6:α-syn ratio of 1:4; Supplementary Fig. 2C).

In order to further elucidate how the interaction of HSPBs influences α-syn lipid-induced aggregation we incubated DMPS SUVs with α-syn monomers and/or HSPBs at the fixed temperature of 30 °C for 4 h and we measured DPH fluorescence polarisation. As previously reported[6,7], co-incubation of α-syn with DMPS SUVs decreased the DPH fluorescence polarization, which corresponds to an increase of their fluidity (Fig. 3A, compare black column to brown column). When incubated alone with DMPS SUVs, HSPB7 and HSPB8 slightly increased the DPH fluorescence polarization; a similar result was obtained upon co-incubation with α-syn (Fig. 3A, purple and grey columns). By contrast, HSPB3 and HSPB5 slightly decreased the DPH fluorescence polarization of DMPS SUVs in absence of α-syn, while increasing it in presence of α-syn (Fig. 3A, dark blue and light blue columns). Finally, HSPB6 strongly decreased the DPH fluorescence polarization of DMPS SUVs in absence and presence of α-syn (Fig. 3A, green columns).

These data confirm the importance of lipids in the mechanism of action of HSPB6 and support the idea that HSPBs reduce α-syn lipid-induced aggregation with distinct mechanisms of action. Plausible mechanisms of action that may explain our results include: 1) HSPB binding to free α-syn monomers, thereby inhibiting their embedding into the lipids; 2) HSPB binding to lipid-bound α-syn, thereby shielding it from oligomerization and further aggregation (Fig. 3B). Concerning HSPB6, it has been shown that transient complex between α-syn monomers and free lipid molecules, which are in equilibrium with the lipid vesicles, may form. These lipid−α-syn complexes are water-soluble and have increased hydrophobicity; this, in turn, enhances their insertion in the lipid membranes, promoting the growth of amyloid fibrils on the lipid membrane surfaces[41]. By binding to either free lipids or lipid membranes, HSPB6 may prevent the formation of these transient water-soluble lipid−α-syn complexes, decreasing the binding affinity of α-syn for lipids and delaying the fibril growth.

**Phosphorylation of serine HSPB6 enhances its inhibitory effect on α-syn lipid-induced aggregation**

HSPB6 is the only member of the HSPB family that contains a RRXS consensus sequence recognized by the protein kinases PKA and PKG[60]. The HSPB6 RRXS motif contains serine residue 16 (S16), which can be phosphorylated by cAMP-PKA and has been implicated in the regulation of HSPB6 interactions and functions, including smooth muscle relaxation and cardioprotection[61]. pS16-HSPB6 promotes its binding to the 14-3-3 protein, competing with the actin depolymerizing protein cofilin[62,63]. Displacement of cofilin from 14-3-3 by pS16-HSPB6 has been suggested to modulate actin dynamics, ultimately favouring actin depolymerization and smooth muscle relaxation[63].

Interestingly, 14-3-3 also interacts with α-syn to reduce its aggregation in vitro and in cells, acting at the level of preformed fibrils and aggregation intermediates[64]. Recently, it has been suggested that 14-3-3 protein buffers exceeding amounts of α-syn at cholesterol rich sites, preventing lipid-induced oligomerization[65]. Whether it does so alone or acting in concert with other binding partners is currently unknown. Based on these premises, here we investigated whether S16-HSPB6 can inhibit α-syn lipid induced aggregation as efficiently as non-phosphorylated HSPB6. To ascertain the impact of HSPB6 phosphorylation *per se*, we conducted these experiments in absence of 14-3-3. We generated non-phosphorylatable HSPB6, by replacing serine 16 with an alanine (S16A) and pseudophosphorylated HSPB6, by replacing serine 16 with aspartic acid (S16D). We also replaced serine 16 with a cysteine residue (S16C), followed by a chemical addition of the phosphate (P) group to generate a phosphorylated S16C-HSPB6 (S16C-P) (Supplementary Fig. 3A-D). We next tested their efficacy in inhibiting α-syn lipid-induced aggregation, using the ThT fluorescence assay and a starting HSPB:α-syn ratio of 1:200. While non-phosphorylatable S16A prevented the α-syn lipid-induced aggregation with an efficacy similar to that of HSPB6 wild-type, pseudophosphorylated S16D and chemically phosphorylated S16C-P showed a stronger inhibitory effect (Fig. 4A,B). Similar results were obtained increasing the HSPB:α-syn ratio to 1:400,

further confirming that, in absence of 14-3-3, HSPB6 Serine 16 phosphorylation slightly enhances its inhibitory effect towards α-syn lipid-induced aggregation (Fig. 4C,D). Dimers of phosphorylated HSPB6 interact with dimers of 14-3-3 [66], with a micromolar affinity in the case of the 14-3-3 ζ isoform [67]. Future studies should investigate whether co-incubation of S16-HSPB6 with different 14-3-3 isoforms influences its ability to prevent α-syn lipid-induced aggregation at cholesterol rich sites.

**HSPB3, HSPB5 and HSPB7 delay α-syn fibril elongation**

Upon assembly, α-syn fibrils grow by elongation, which can be measured using ThT fluorescence by incubating at neutral pH preformed fibrils with free α-syn monomers in absence of SUVs (Figure 1, middle panel)[6,7,11]. With this elongation assay, we tested the efficacy of HSPBs to prevent α-syn fibril growth, using different HSPBs:α-syn ratios. The results obtained with this assay, in absence of lipids, will be instrumental for the interpretation of the ones obtained using the α-syn lipid-induced aggregation assay. Importantly, in this fibril elongation assay we used 1 μM of α-syn seeded fibrils, 20 μM of α-syn monomers and progressively decreasing concentrations of HSPBs, thus enabling us to extrapolate the affinity of HSPBs towards the preformed fibril extremities versus the free α-syn monomers (in large excess compared to the preformed fibrils). At the 1:1, 1:2 and 1:4 HSPBs:α-syn ratios, all HSPBs tested delayed the elongation of α-syn preformed fibrils, although with different kinetics (Fig. 5A-C). To enable direct comparison of the efficacy of the HSPBs, the measured elongation rates were normalised relative to the one of α-syn alone (Fig. 5D). HSPB3, HSPB5 and HSPB7 inhibited α-syn elongation with a relative fibril elongation ratio of approximately 0.1, independently of the HSPBs:α-syn ratio. HSPB8 delayed fibril elongation with a relative fibril elongation ratio of 0.2 to 0.6, based on HSPB8 concentration: the lower HSPB8 concentration (1:4 ratio), the lower the efficacy (Fig. 5D). Concerning HSPB6, its efficacy in inhibiting α-syn fibril elongation was poorer compared to the one of HSPB8 (Fig. 5D); of note, when HSPB6 concentration was 4-times lower than the one of monomeric α-syn, HSPB6 had almost no effect (Fig. 5D, 1:4 ratio).
Of note, the lipid-induced aggregation assay was performed using higher HSPBs:α-syn ratios, ranging from 1:100 and 1:400 (Figure 2). We then repeated the experiments lowering further the concentration of HSPBs and using 1:20, 1:50, 1:100 and 1:200 HSPBs:α-syn ratios (Fig. 5E-I), enabling the comparison between the efficacy of HSPBs in preventing α-syn aggregation in absence and presence of lipids. HSPB3, HSPB5 and HSPB7 could still efficiently delay α-syn fibril elongation even at the highest 1:200 ratio, while HSPB6 was completely inactive at the higher ratios and showed only poor activity at the 1:20 ratio (Fig. 5E-H). By contrast, at the 1:200 ratio, HSPB6 was by far more efficient in preventing monomeric α-syn lipid-induced aggregation. Concerning HSPB8, its efficacy was concentration-dependent and progressively decreased with increasing amounts of free α-syn monomers, being lost at the highest ratio (Fig. 5I). Based on these data, we conclude that HSPB3, HSPB5 and HSPB7 efficiently prevent fibril elongation, in a wide concentration. This observation suggests that they would bind with higher affinity to the fibril surface and extremities, rather than to free α-syn monomers (Fig. 5J). Of note, previous work identified higher binding affinity of HSPB5 for the length of the fibril and lower affinity for the fibril ends [54,68]. Instead, HSPB8, whose efficacy is dose-dependent and decreases with increasing concentrations of free α-syn monomers, would preferentially bind to the latter (Fig. 5J). Finally, the comparison of the results obtained at the higher ratios 1:100 and 1:200 in absence and presence of lipids supports the idea that HSPB6 interacts weakly with monomeric α-syn (Fig. 5J), and acts instead as a lipid-dependent molecular chaperone.

**HSPB3 and HSPB7 inhibit the rate of α-syn fibril amplification under mildly acidic pH**

We next tested the ability of HSPBs to inhibit the formation of α-syn higher order assemblies, which have been observed to occur via secondary nucleation upon incubation of α-syn fibrils and free monomers at mildly acidic pH[11,69] (Fig. 1, right panel). Since the secondary nucleation assay is performed at pH 5.5, we studied the folding and stability of the various HSPBs at acidic pH using circular dichroism (CD). Previous work showed that HSPB5 is sensitive to pH changes. Lowering the pH from 7.5 to 6.5 promotes dimer to monomer dissociation and the formation of polydisperse oligomers with increased holdase capacity[70]. However, lowering the pH from 6.5 to

5.5 affected the CD spectra of HSPB5, suggesting protein destabilization, which may in turn affect its chaperone function (Supplementary Fig. 4B). Due to the high sensitivity to lower pH and to avoid data misinterpretation, we did not assess HSPB5 efficacy in inhibiting secondary nucleation at mildly acidic pH. Instead, the CD spectra of HSPB3, HSPB6, HSPB7 and HSPB8 were similar regardless of the acidic pH (Supplementary Fig. 4A, C-E), enabling us to study their efficacy in inhibiting α-syn secondary nucleation at pH 5.5. The secondary nucleation assay consists in the acquisition of ThT fluorescence upon co-incubation at pH 5.5 of 50 nM α-syn seeded fibrils, 20 μM α-syn monomers and progressively decreasing concentrations of HSPBs. The use of a large excess of α-syn monomers compared to the preformed fibrils enables to gain insights into HSPB affinity on the different states of α-syn. To quantify differences in the efficacy of the HSPBs, we performed the measures using three HSPBs:α-syn ratios: 1:1, 1:2 and 1:4. HSPB3 and HSPB7 strongly inhibited α-syn secondary nucleation regardless of the ratio used (Fig. 6A-C). HSPB8 showed a moderate and dose-dependent effect, while HSPB6 showed the lowest efficacy compared to the other members of the family tested (Fig. 6A-C). Similar to what we observed using the elongation assay (Fig. 5I), HSPB8 chaperone activity inversely correlated with the concentration of free α-syn monomers (Fig. 6D), suggesting that HSPB8 inhibits α-syn aggregation by preferentially binding to and neutralizing its monomeric forms. By contrast, HSPB3 and HSPB7, whose efficacy is not influenced by the presence of exceeding monomeric free α-syn, would preferentially bind to α-syn fibrils (Fig. 6D), in agreement with the observations from the elongation assay.

**The inhibitory effect of HSPB6 on α-syn lipid-induced aggregation correlates with its affinity for lipids**

The integrated analysis of the results obtained in absence (Figs. 5 and 6) and presence of DMPS SUVs (Figs. 2 and 3) revealed that HSPB6 chaperone activity depends on the presence of lipid membranes. In order to better understand how different lipid types can influence the chaperone activity of HSPB6, and considering that α-syn can interact with different types of biological membranes, we generated membrane-mimetic SUVs with lipid composition that resemble either the outer leaflet of the plasma membrane (PM), the inner leaflet of the PM, the mitochondrial, the ER or the Golgi membranes (Fig. 7A and Supplementary Fig. 5). Of note, these membrane-mimetic SUVs are composed of longer fatty acid chains (> 18:0) compared to DMPS vesicles (14:0), conferring properties that are similar to the ones of physiological cellular and organelle membranes. We then studied whether these different types of lipids influence HSPB6 efficacy in preventing α-syn lipid-induced aggregation. The choice of these membrane-mimetic SUVs was driven by published data indicating that α-syn, which was initially identified as a protein enriched in the presynaptic terminal, where it associates with synaptic vesicles[71,72], can bind to a large variety of lipid membranes, including the plasma membrane, mitochondrial membranes, lipid rafts and caveolae, as well as ER and Golgi membranes[73,74]. Interaction with these lipid membranes, which occurs with different strengths based on their lipid composition, is important for α-syn physiological functions, but it is also tightly associated with α-syn pathological effects. For example, α-syn has a strong affinity for mitochondrial membranes[75] and excessive binding of α-syn to these lipid membranes leads to neuronal toxicity[76]. In addition, excessive association of α-syn with ER and Golgi impairs vesicular trafficking, promotes Golgi fragmentation and leads to the depletion of lysosomal enzymes in cellular and Drosophila models of PD[77]. Finding that the efficacy of HSPB6 in inhibiting α-syn lipid-induced aggregation correlated with HSPB6 binding affinity to the lipid membranes suggests that it may protect different lipid membrane types from α-syn induced damage. In addition, it helps dissecting its mechanism of action. Currently, two mechanisms of action could be compatible with the results observed: competition with α-syn for binding to lipids (either as α-syn monomers or transient α-syn-lipid water-soluble complexes), and binding to α-syn monomers embedded into the lipids, thus shielding then from further oligomerization/aggregation. Future studies will need to address the question whether by binding to lipids HSPB6 changes their order, indirectly influencing α-syn binding to lipids.

First, we measured the affinity of α-syn for the different membrane-mimetic SUVs and we calculated the fraction of α-syn bound to increasing concentrations of lipids. In agreement with previous findings[75], α-syn had the highest affinity for the mitochondrial membrane compared to the other membrane-mimetic SUVs (Fig. 7B). In

particular, α-syn showed the lowest affinity for SUVs mimicking the outer PM, and an intermediate affinity for SUVs mimicking the inner PM, Golgi and ER (Fig. 7B). Second, we measured the affinity of HSPB6 for the different membrane-mimetic SUVs. HSPB6 showed the highest binding affinity for SUVs mimicking the inner PM, followed by the outer PM and mitochondria (Fig. 7C); the weakest interaction was detected for SUVs mimicking the composition of ER and Golgi membranes (Fig. 7C).

We then evaluated the ability of HSPB6 to inhibit α-syn lipid-induced aggregation in presence of these different membrane-mimetic SUVs, using the ThT fluorescence assay and different HSPB6:α-syn ratios (Fig. 7D-H). At a 1:100 ratio, HSPB6 abrogated α-syn lipid-induced aggregation regardless the lipid types employed (Fig. 7D-H, compare green line with black line), while at the highest 1:800 ratio, HSPB6 lost its inhibitory effect under all conditions tested (Fig. 7D, compare red line with black line). Instead, at the 1:200 and 1:400 ratios, HSPB6 delayed lipid-induced aggregation with efficiencies that varied based on the SUV composition (Fig. 7D-H, compare brown and orange lines with black line). We then calculated the normalized aggregation half time (t1/2) at the 1:200 ratio and we correlated it (y-axis) with the binding affinity for lipids (Kd, x-axis), followed by analysis of the Pearson's correlation coefficient (Figure 7I). This analysis revealed a significant correlation (r=0.85, p-value 0.0375) between the binding affinity of HSPB6 for lipids and its efficacy in preventing α-syn lipid-induced aggregation. The strongest inhibitory effect was exerted by HSPB6 in presence of SUVs that mimic the inner PM, followed by the outer PM and mitochondria. The lowest inhibitory effect of HSPB6 was observed when using SUVs that mimic the Golgi and the ER (Fig. 7I), for which HSPB6 lipid-binding affinity was the lowest (Fig. 7C). These data support the idea that HSPB6 is a lipid-dependent molecular chaperone.

**Discussion**

As α-syn aggregates are central to synucleopathies, tremendous efforts have been made to understand in detail the process of α-syn aggregation in order to identify effective ways to combat it. Achieving this goal is challenging because different paths lead to the formation of α-syn aggregates, including lipid-induced aggregation and α-syn liquid-liquid phase separation, followed by liquid-to-solid conversion[19]. Moreover, environmental factors, such as pH, can accelerate specific steps of the aggregation process[6,7,69].

Molecular chaperones, namely HSPs, have been for long considered as ideal candidates to prevent protein aggregation[78]. Although much progress has been made in understanding molecular mechanisms of action of HSPs, and substantial evidence has been accumulated demonstrating their efficacy in blocking α-syn aggregation, the majority of the studies carried out to date have focused on a protein-centric view, so that several questions remain open on whether and how lipid membranes may influence the chaperone activity of HSPs[23,25,50,79]. Here we have focused on the mammalian HSPB family, providing evidence that HSPBs evolved to block with multiple points of attack the kinetic network of microscopic processes leading to protein aggregation, with HSPB6 emerging as a lipid-dependent molecular chaperone.

In presence of lipid membranes, HSPB6 was by far more efficient than the other members of the family in preventing α-syn lipid-induced aggregation (Fig. 2 and 3). By contrast, in absence of lipid membranes, HSPB6 showed a poor chaperone activity, whereas HSPB3, HSPB5 and HSPB7 were very efficient in preventing α-syn elongation, even at low concentrations (Fig. 5) or at mildly acidic pH (Fig. 6). Mechanistically, secondary nucleation consists of the fibril-dependent generation of new aggregates[80]. These aggregates, in turn, elongate by addition of α-syn monomers and serve as a platform that amplifies α-syn aggregation[80]. Previous reports showed that HSPBs can associate with fibrils during the aggregation process, delaying the process and affecting the morphology of the fibrils. The fibrils formed in presence of HSPBs were either similar but fewer in number (with HSPB5), shorter (with HSPB1 or HSPB2-HSPB3 complex) or no fibrils, but compact structures formed (with HSPB8)[28]. Using a high concentration of α-syn monomers compared to that of preformed fibrils, and progressively decreasing the concentration of the HSPBs tested enabled us to identify preferential binding of

HSPB8 to monomeric versus fibrillar α-syn. This may help explain why HSPB8 changes the morphology of α-syn aggregates. Instead, HSPB3, HSPB5, HSPB7, whose efficacy was maintained regardless of the concentration of monomeric free α-syn, preferentially bound to pre-formed fibrils (Figs. 5 and 6). Given that also HSPB1 and HSPB5 bind to α-syn fibrils[26,30,50,54,68], binding to and coating the fibrils, yielding shorter or fewer fibrils, as previously reported[28], would represent a general mechanism by which HSPB combat aggregation. Instead, buffering free α-syn monomers and preventing their incorporation onto the fibril surface seems to be the preferred mechanism of action for HSPB8 (Figs. 5 and 6), while acting at the α-syn protein-lipid interface appears as the action of choice for HSPB6 (Figs. 2-4). Intriguingly, HSPB8 shows the highest disorder and the highest propensity to undergo liquid-liquid phase separation, compared to the other HSPB members [17] and was previously shown to prevent the aggregation of the RNA binding protein FUS inside condensates by chaperoning its aggregation-prone RNA binding domain [21]. These observations suggest that HSPB8 could also co-condense with α-syn, in addition to interacting with the pre-formed fibrils as investigated in our work, preventing the maturation of α-syn condensates into amyloid aggregates. Concerning HSPB6, finding that its chaperone activity towards α-syn is lipid-dependent may explain why previous studies failed to identify any effect of HSPB6 on fibril morphology and only a minor effect on α-syn fibril formation[28], defining HSPB6 as a poor chaperone compared to the other members of the family.

We note that we still do not fully understand what regulates the lipid-dependent chaperone activity of HSPB6. At the highest HSPB:α-syn ratios, all HSPBs tested could efficiently delay α-syn-lipid induced aggregation, revealing a novel general mode of action for HSPBs at the protein-lipid interface. The ability of HSPBs to interact with lipids and prevent α-syn lipid-induced aggregation might be influenced by their degree of disorder. Of note, lipid binding is common among disordered proteins [81] and HSPBs contain N-terminal and C-terminal intrinsically disordered domains[42]. In addition, prion domains exhibit membrane binding propensities[82]; thus, the predicted prion-like domains in the HSPB protein sequence (http://plaac.wi.mit.edu/) may also enhance their binding affinity for lipids. Rather than a specific sequence, the structural heterogeneity of multiple coexisting conformations of HSPBs may be responsible for their binding to lipids. Binding to specific lipid types could transiently lock the HSPB molecules in an active conformation, similar to what happens upon post-translational modifications, influencing their chaperone activity. This inherent structural heterogeneity may explain why most HSPBs show efficient chaperone activity in absence of lipids, while HSPB6 binding to lipids would be required to unlock its chaperone power and prevent α-syn aggregation. The findings that the fluorescence polarization of DPH decreases in presence of HSPB6 or α-syn alone and further decreases when both proteins are co-incubated with SUVs (Fig. 3 and Supplementary Fig. 1) support the idea that HSPB6 directly interacts with lipid membranes. We cannot exclude the possibility that HSPB6 may bind to free lipids in equilibrium with the SUVs; in doing so, HSPB6 may decrease the formation of transient water-soluble lipid−α-syn complexes, ultimately reducing their incorporation into the lipid membranes. Alternatively, the changes in lipid membrane viscosity induced upon HSPB6 binding to them may change the local biophysical properties of the lipid membranes themselves, reducing the binding affinity of α-syn monomers. Another possible mechanism is that HSPB6 may bind to monomeric α-syn embedded into the lipid membranes, acting as a shield that would prevent aggregation. Yet, HSPB6 was shown to weakly and transiently bind to monomeric α-syn[28]. Considering that the efficacy of HSPB6 in inhibiting α-syn lipid-induced aggregation correlates with its binding affinity for the lipids themselves (Fig. 7), and in light of its poor chaperone ability in the absence of lipids and in the presence of excess monomeric α-syn (Fig. 5, 6) [83,84], we favor the hypothesis that HSPB6 acts as a lipid-dependent molecular chaperone that interferes with α-syn embedding into the lipids. These data open the possibility that HSPB6 may preferentially inhibit the aggregation of fibril-forming proteins that bind to lipids.

This work informs on the importance of exploiting HSPB6 lipid-binding properties for the development of future therapeutic approaches in synucleopathies. HSPB6 is expressed throughout the brain, including the hippocampus, amygdala, cerebral cortex and basal forebrain that degenerate in the advanced stages of PD[85], is upregulated in hippocampal neurons subjected to oxidative and hyperosmotic stress[86] and exerts

neuroprotective functions in vivo[87]. Of note, HSPB1 and HSPB5 were also able to reduce α-syn lipid-induced aggregation, although with a lower efficacy compared to HSPB6. Considering that HSPB1 and HSPB5 are upregulated in the brain of patients affected by PD and other neurodegenerative diseases[88,89], we cannot exclude the possibility that their neuroprotective effects could be due, at least in part, also to the inhibition of lipid-induced protein aggregation.

Although it is still unclear where exactly α-syn lipid-induced aggregation occurs inside the cells, previous reports highlighted the mitochondria as the preferred subcellular site[76]. The association of aggregated α-syn with mitochondria increases the production of toxic reactive oxygen species and impairs cellular respiration[76]. In addition, transcellular propagation of α-syn aggregates, similar to prion protein aggregates, and impairment of membrane fusion events at synaptic terminals are well-established mechanisms contributing to synucleopathies[90]. Of note, the membrane binding properties of α-syn are important for its internalization and spreading[91]. HSPB6 interacts both with lipid vesicles mimicking mitochondrial and plasma membranes (Fig. 7). Thus, increasing HSPB6 expression could protect not only mitochondria from α-syn-mediated toxicity, but also prevent α-syn transcellular propagation.

In summary, our data support the view that protein aggregation takes place by a complex non-linear network of interconnected processes that are influenced not only by protein-protein interactions, but also by protein-lipid interactions. Recently, sharp and reversible transitions were described in the cell membranes of living neurons, further supporting their biological relevance for e.g. signal transduction and excitability[92]. It is tempting to speculate that the direct interaction of the HSPBs with lipid membranes, supported by DPH fluorescence anisotropy measurements, and in agreement with previous studies[35,93-96], may contribute to stabilize the membranes upon stress conditions that influence membrane integrity and fluidity, such as heat shock and the presence of aggregation-prone proteins. Future studies will need to address to what extent the cytoprotective functions of HSPs are related to, or perhaps even dependent on, interactions with lipids. Our results indicate that HSPBs may have evolved to diversify their efficacy in a context-dependent manner, with some members becoming active only in presence of lipid membranes, and acting in different subcellular environments, both in solution and in phase-separated environments. These emerging properties may explain why, amongst the numerous molecular chaperones, small HSPs are highly represented in organisms exposed to extreme stressful conditions such as tardigrades[97], and why HSPBs are specifically upregulated in humans during aging, when the general protein homeostasis system declines[78].

**Limitations of the Study**

While our study provides valuable insights into the interactions between HSPBs and α-syn, several limitations must be acknowledged. Interaction with lipid vesicles: Recent studies have shown that the binding of α-syn to model cell membranes that contain negatively charged lipids induces reversible structural changes that promote the formation of rod-like or disc-like lipid-protein particles[98]. The small particles containing α-syn and lipids resulting from the fast and reversible rupture of the lipid vesicles can then be incorporated into the fibrils[98]. This mechanism has been suggested to contribute to the formation of the pathological protein-lipid aggregates found in PD patients. In our work we did not test whether/how HSPBs may influence the structural re-arrangements of the lipid vesicles into small particles. Future work should establish whether HSPBs affect the formation of specific discs or rods protein-lipid phases, thereby decreasing the frequency of unfavorable protein-protein interactions that facilitate amyloid fibril formation. Despite this limitation, we conclude that the interactions with lipids of HSPBs (especially HSPB6) can influence their anti-aggregation activity towards α-syn. Specificity of lipid interactions: The interactions of HSPBs, especially HSPB6, with a wider range of lipid membranes were not fully characterized. While we established that HSPB6 acts as a lipid-dependent molecular chaperone, further research is needed to determine the specific lipid compositions that most effectively modulate this chaperone activity. Understanding these specific interactions could provide deeper insights into the mechanisms by which HSPBs

stabilize membranes and prevent protein aggregation. Environment-dependent activity: Our study suggests that some HSPBs may become particularly active in the presence of lipid membranes, acting differently in various subcellular environments. However, the context-dependent efficacy of these molecular chaperones was not exhaustively investigated across all possible cellular conditions. Further studies will be needed to confirm these findings in diverse cellular and in vivo models to validate the proposed mechanisms. Mechanistic insights: While we propose that HSPBs might stabilize cell membranes and reduce amyloid fibril formation by influencing lipid-protein interactions, the corresponding molecular mechanisms remain to be fully elucidated. Detailed biophysical and structural studies will be required to characterize the precise ways in which HSPBs interact with lipid membranes and α-syn aggregates at the molecular level. In vivo relevance: Since our findings are based on in vitro assays, their in vivo relevance will require further validation. Animal models and clinical studies will be necessary to confirm the protective roles of HSPBs, particularly HSPB6, in neurodegenerative diseases, including Parkinson's disease. Comparative analysis: The study focused on a subset of HSPBs, finding that they have different relative efficacy in preventing α-syn aggregation. Future research should include a broader range of HSPBs to determine if other members of this family exhibit similar, or perhaps, superior anti-aggregation properties, as well as lipid-dependent chaperone activity.

**ACKNOWLEDGMENTS**

We acknowledge Prof. J. Buchner for providing the vectors coding for HSPB3-5-6-7 [84]. We acknowledge Greta Šneiderienė for technical help with binding affinity measurements. S.C. acknowledges for funding MUR (Departments of excellence 2018-2022; E91I18001480001), University of Modena and Reggio Emilia (FAR2020), Telethon Foundation (GGP15001 and GMR22T1003) and AriSLA Foundation (SUMOsolvable); M.V. acknowledges for funding the Centre for Misfolding Diseases (University of Cambridge). We acknowledge support from the Centre for Misfolding Diseases (University of Cambridge) and UKRI (grants 10059436 and 10061100).

**AUTHOR CONTRIBUTIONS**

S.C. (Serena Carra) and M.V. conceived the study. V.S and T.T. performed the experiments and carried out the analyses with the assistance of R.S., S.P. and S.C. (Sean Chia). S.C. (Serena Carra) and M.V. wrote the paper with input from all authors.

**DECLARATION OF INTERESTS**

M.V. is a founder of WaveBreak Therapeutics (formerly Wren Therapeutics). The other authors declare no competing interests.

**Figure Legends**

**Figure 1. Schematics of the three-pronged approach used to characterise α-syn aggregation.** Three different assays were used to probe: (left) lipid-induced aggregation, where monomeric α-syn forms growth-competent nuclei due to the interaction with lipid surfaces; (center) elongation, where monomeric α-syn interacts with existing preformed fibrils at high concentrations (high seed) and pH 6.5, forming longer fibrils; (right) secondary nucleation, where monomeric α-syn interacts with existing preformed fibrils at low concentrations (low seed) and pH 5.5. Secondary nucleation refers to a surface catalyzed mechanism that leads to the formation of toxic oligomeric species in the presence of amyloid fibrils. This process is accelerated at mildly acidic pH, generating new fibrils and new oligomeric species[6,7,11].

**Figure 2. HSPBs inhibit lipid-induced α-syn aggregation.** (A) Changes in ThT fluorescence intensity when monomeric α-syn (20 μM) is incubated with 100 μM DMPS vesicles at pH 6.5 and 30 °C (DMPS:α-syn ratio is 5:1)

and in the absence (black) or presence of HSPBs (colored lines) at the following HSPB:α-syn ratios: 1:100 (0.2 μM:20 μM) (A), 1:200 (0.1 μM: 20 μM) (C), 1:400 (0.05 μM:20 μM) (E) and 1:50 (0.4 μM: 20 μM) (G). Data are presented as absolute ThT fluorescence. a.u. arbitrary units. (B, D, F) Comparison of α-syn aggregation half-time in absence/presence of HSPBs, as per conditions detailed in A, C and E, respectively. Data are shown as mean ± sem. n = 3 independent experiments. One-way ANOVA, followed by Bonferroni-Holm *post-hoc* test. Comparison between α-syn alone or with each HSPB is shown.

**Figure 3. Impact of HSPBs on the fluidity of DMPS lipid vesicles and on α-syn lipid-induced aggregation.** (A) Changes in DMPS (100 μM) membrane fluidity due to presence of α-syn or HSPBs (20 μM) detected through fluorescence polarization of DPH at 30 °C for 4 h (DMPS:α-syn and DMPS:HSPB ratio are 5:1). Data are shown as mean ± sem. n = 3 independent experiments. One-way ANOVA, followed by Bonferroni-Holm post-hoc test. Comparison between DPH fluorescence polarization of DMPS alone or with α-syn and/or each HSPB studied are shown. (B) Putative mechanisms of action of HSPBs towards α-syn lipid-induced aggregation. HSPBs could transiently associate with α-syn monomers, hence preventing their binding to lipid membranes. In addition, and not mutually exclusive, HSPBs could interact with lipid-bound α-syn, thereby shielding it from aggregation. Furthermore, HSPBs could directly interact with lipids, thus reducing the association of α-syn with lipid membranes. The latter seems to be the preferred mechanism of action of HSPB6.

**Figure 4. S16 phosphorylation enhances the lipid chaperone activity of HSPB6.** (A-D) Changes in ThT fluorescence intensity when monomeric α-syn (20 μM) is incubated with 100 μM DMPS vesicles at pH 6.5 and 30 °C and in the absence (black) or presence of HSPB6 wild-type, non-phosphorylatable HSPB6 (S16A), pseudophosphorylated HSPB6 (S16D) and chemically phosphorylated HSPB6 (S16C-P) at the HSPB:α-syn ratios 1:200 (0.1 μM: 20 μM) (A) and 1:400 (0.05 μM: 20 μM) (C). (B, D) Comparison of α-syn aggregation half-time, in the presence of HSPB6, S16A, S16D or S16C-P as per conditions in detailed in A and C, respectively. Data are shown as mean ± sem. n = 3 independent experiments. One-way ANOVA, followed by Bonferroni-Holm post-hoc test. Comparison between HSPB6 wild-type and either S16A, S16D or S16C-P is shown.

**Figure 5. HSPBs delay α-syn fibril elongation.** (A) Changes in ThT fluorescence intensity when monomeric α-syn (20 μM) is incubated with 1 μM preformed fibrils at pH 6.5 and 37 °C and in the absence (black) or presence of HSPBs at three different HSPB:α-syn ratios: 1:1 (20 μM: 20 μM) (A), 1:2 (10 μM:20 μM) (B) and 1:4 (5 μM:20 μM) (C). Data are reported as absolute ThT fluorescence. a.u. arbitrary units. (D) Relative rate of α-syn fibril elongation, determined as previously described [11]. (E-I) Changes in ThT fluorescence intensity as described in A, but using the following HSPB:α-syn ratios: 1:200 (0.1 μM: 20 μM), 1:100 (0.2 μM: 20 μM), 1:50 (0.4 μM: 20 μM), 1:20 (1 μM: 20 μM). Data are shown as mean ± sem. n = 3 independent experiments. (J) Putative mechanism of action of HSPBs on fibril elongation.

**Figure 6. HSPBs delay α-syn secondary nucleation.** (A-C) Changes in ThT fluorescence intensity when monomeric α-syn (20 μM) is incubated with 50 nM preformed fibrils at pH 5.5 and 37 °C and in the absence (black) or presence of HSPBs at three different HSPB:α-syn ratios: 1:1 (20 μM: 20 μM) (A), 1:2 (10 μM:20 μM) (B) and 1:4 (5 μM:20 μM) (C). Data are shown as absolute ThT fluorescence. a.u. arbitrary units. Data are shown as mean ± sem. n = 3 independent experiments. (D) Putative mechanism of action of HSPBs on secondary nucleation.

**Figure 7. The binding affinity of HSPB6 for different lipid types influences the inhibition of α-syn lipid-induced aggregation.** (A) Composition of membrane-mimetic SUVs resembling mitochondria membrane, the outer PM, the inner PM, the ER or Golgi membranes. (B) Binding affinity of α-syn (5 μM) for each membrane-mimetic SUV, expressed as fraction bound. Dissociation constant (Kd) values are as follows: 0.069 for mitochondria; 0.119 for outer PM; 0,082 for inner PM; 0.104 for ER; 0.104 for Golgi. (C) Binding affinity of HSPB6 (5 μM) for each membrane-mimetic SUVs, expressed as fraction bound. Dissociation constant (Kd) values are as follows: 0.072 for mitochondria; 0.062 for outer PM; 0.045 for inner PM; 0.095 for ER; 0.088 for Golgi. (D-H). Changes in ThT

fluorescence intensity when monomeric α-syn (20μM) is incubated with 100 μM of membrane-mimetic SUVs at pH 6.5 and 30 °C and in the absence (black) or presence of HSPBs (colored lines) at the following HSPB:α-syn ratios: 1:100 (0.2 μM:20 μM), 1:200 (0.1 μM:20 μM), 1:400 (0.05 μM: 20 μM), 1:800 (0.025 μM: 20 μM). (I) Correlation of the binding affinity of HSPB6 for lipids (Kd, x-axis) with the half-time of aggregation at the 1:200 ratio (y-axis), followed by analysis of the Pearson's correlation coefficient (r): r = 0.85; p = 0.0375. Data are shown as mean ± sem. n = 3 independent experiments.

**STAR METHODS**

Detailed methods are provided in the online version of this paper and include the following:

**KEY RESOURCES TABLE**

**RESOURCE AVAILABILITY**

Lead contact

Materials availability

Data and code availability

**METHOD DETAILS**

Protein production

Lipid vesicle preparation

Site-directed mutagenesis

Generation of an HSPB6 phosphorylation mimetic

Far-UV circular dichroism (CD) spectroscopy

Preparation of α-syn seed fibrils

Measurements of aggregation kinetics (ThT assay)

Labeling α-syn and HSPB6

Binding affinity assay

Statistical analyses

Analysis of the aggregation kinetics

**QUANTIFICATION AND STATISTICAL ANALYSIS**

**SUPPLEMENTAL INFORMATION**

Supplemental information contains supplemental materials and methods, five supplemental figures and references.

## STAR*METHODS

### Key resources table

| REAGENTS OR RESOURCE | SOURCE | IDENTIFIER |
|---|---|---|
| **Chemicals, peptides, and recombinant proteins** | | |
| Complete™, EDTA-free Protease Inhibitor Cocktail | Roche | 11873580001 |
| IPTG | Invitrogen | 15529-019 |
| Benzonase 250 U/mL | Sigma-Aldrich | E8263-5ku |
| Arabinose | Lucigen | 490234 |
| GsH | Sigma-Aldrich | G4251 |
| Thioflavin T UltraPure Grade | Eurogentec | AS-88306 |
| $NaH_2PO4$ , BioPerformance Certified > 99.0% | Sigma-Aldrich | S6191 |
| $Na_2HPO4$, ReagentPlus, > 99.0% | Sigma-Aldrich | S0876 |
| NaN3, ReagentPlus, >99.5% | Sigma-Aldrich | S2002 |
| PC: L-α-phosphatidylcholine | Avanti Polar Lipids | 840053P-25mg |
| PE: L-α-phosphatidylethanolamine | Avanti Polar Lipids | 840022P-25mg |
| PI: L-α-phosphatidylinositol-4-phosphate | Avanti Polar Lipids | 840045p-25mg |
| PS: L-α-phosphatidylserine | Avanti Polar Lipids | 840032P-25mg |
| SM: Sphingomyelin | Avanti Polar Lipids | 860062P-25mg |
| chol: cholesterol | Avanti Polar Lipids | 700100P-100mg |
| DMPS (1,2-Dimyristoyl-sn-glycero-3-phospho-L-serine) sodium salt | Avanti Polar Lipids | 840033 |
| Diphenylhexatriene (DPH) | Sigma-Aldrich | SML0202 |
| HEPES | Sigma-Aldrich | H3375 |
| DTT | Sigma-Aldrich | D0632 |
| NaCl | Sigma-Aldrich | S3014 |
| KCl | Sigma-Aldrich | P3911 |
| Sodium Phosphate dibasic | Sigma-Aldrich | S9763 |
| Potassium Phosphate monobasic | Sigma-Aldrich | P0662 |
| α-synuclein | This paper | N/A |
| HSPB3 | This paper | N/A |
| HSPB5 | This paper | N/A |
| HSPB6 | This paper | N/A |
| HSPB7 | This paper | N/A |
| HSPB8 | This paper | N/A |
| **Bacterial and virus strains** | | |
| Escherichia coli strain BL21 | Thermo Fisher | C607003 |
| **Plasmid** | | |
| pET21a-HSPB3 | Mymrikov et al. [84] | N/A |
| pET23b-HSPB7 | Mymrikov et al. [84] | N/A |
| pET28b(+)-HSPB5 | Mymrikov et al. [84] | N/A |
| pUBS520-HSPB6 | Mymrikov et al. [84] | N/A |
| pGEX-4T-GST-HSPB8 | Carra et al. [99] | N/A |
| **Software and algorithms** | | |
| Prism 8 (GraphPad) | GraphPad Software | https://www.graphpad.com/ |
| Daniel's XL Toolbox | open-source add-in for Microsoft® Excel® | https://www.xltoolbox.net/ |
| **Other** | | |

| | | |
|---|---|---|
| Sephacryl S300 High-Prep 16/60 column | GE Healthcare | 745515 |
| Superdex 200-pg column | GE Healthcare | 28-9893-36 |
| Protino GST/4B Column | Macherey-Nagel | 745515.5 |
| High-Trap Q HP column | GE Healthcare | 17-1154-01 |

## RESOURCE AVAILABILITY

### Lead contact

Further information and requests for reagents should be directed to and will be fulfilled by the lead contact, (serena.carra@unimore.it).

### Materials availability

Cell lines generated in this study will be available upon reasonable request from the lead contact.

### Data and code availability

• Any additional information required to reanalyze the data reported in this paper is available from the lead contact upon request.

• All data reported in this paper will be shared by the lead contact upon request.

• This paper does not report original code.

## METHOD DETAILS

### Protein production

α-syn wild-type and α-syn cysteine variant (N122C) were expressed and purified as previously described[80]. Briefly, *E. coli* strain BL21 competent cells were transformed with pT7-7 plasmid coding wild type human α-syn. Protein expression was performed by addition of 1 mM isopropylβ-thiogalactopyranoside (IPTG, Merck) at 30°C for 4 h. Following purification, the purity of the aliquots was evaluated by SDS–PAGE and we used an extinction coefficient of 5600 $M^{-1}$ $cm^{-1}$ at 275 nm for protein concentration measurements. The protein solutions were aliquoted, flash frozen in liquid nitrogen and stored at -80°C, until required for use. Human small heat shock proteins were expressed in *E. coli* BL21(DE3) and purified as described elsewhere[84]. Before use, proteins were dissolved or diluted in a phosphate buffer and dialyzed if necessary. Protein concentrations were calculated based on their absorbance values at 275 nm, with an extinction coefficient reported by the UniProt database.

### Lipid vesicle preparation

Lipid powders (Avanti lipids) were dissolved following manufacturer's instruction. 1,2-diacyl-sn-glycero-3-phospho-L-serine (DMPS; 14:0) lipid powder (840033, Avanti Lipids) was suspended in 20 mM phosphate buffer ($NaH2PO4/Na_2HPO_4$), pH 6.5, 0.01% $NaN_3$ and stirred at 45°C (which corresponds to DMPS melting temperature) for 4 h as previously reported [7]. Briefly, the solutions were frozen and thawed five times using dry ice and a water bath at 45°C. Lipid vesicles were prepared by sonication to avoid grains of segregated lipids (Bandelin, Sonopuls HD 2070, 3 x 5 min, 50% cycle, 10% maximum power) and centrifuged at 15,000 rpm for 30 min at 25 °C (Medifuge Small Benchtop Centrifuge, Thermo Scientific). The sizes of the DMPS SUVs were checked using dynamic light scattering (Zetasizer Nano ZSP, Malvern Instruments, Malvern, UK) to consist of a distribution centred at 20 nm diameter. For the preparation of membrane-mimetic SUVs, lipid powders of the following lipids were used: L-α-phosphatidylcholine (840053P), referred to as phosphatidylcholine (PC; average fatty acid distribution: 33.3% 18:1, 30.6% 16:0, 16.5% 18:0, 3.1% 20:4, 4% other, 12.8% unknown), L-α-

phosphatidylethanolamine (840022P), referred to as phosphatidylethanolamine (PE; average fatty acid distribution: 24.1% 18:1, 18.6% 20:4, 15.9% 18:0, 11.5% 22:6, 3.7% 16:0, unknown 21.1%, 5.4% other), L-α-phosphatidylinositol-4-phosphate (840045p), referred to as phosphatidylinositol (PI; average fatty acid distribution: 37.3% 18:0, 33.1% 20:4, 15.2% 18:1, 6.3% 16:0, 8.1% other), L-α-phosphatidylserine (840032P), referred to as phosphatidylserine (PS; average fatty acid distribution: 42% 18:0, 30% 18:1, 11% 22:6, 2% 20:4, 15% unknown), sphingomyelin (860062P), referred to as sphingomyelin (SM; average fatty acid distribution: 50% 18:0, 21% 24:1, 7% 22:0, 5% 24:0, 5% 20:0, 2% 16:0, 10% unknown) and cholesterol (700100P) (Avanti Polar Lipids) were suspended in 20 mM phosphate buffer ($NaH2PO4/Na_2HPO_4$), pH 6.5, 0.01% $NaN_3$ and stirred at 45 °C for 4 h. The membrane-mimetic SUVs were prepared by mixing in different combinations and percentage the different lipid types (as detailed in Fig. 7A), as previously described [100]. SUVs were used for the experiments immediately after dispersion and verification of their homogeneous size.

**Site-directed mutagenesis**

Vectors coding for phosphomimicking (S16D) and non-phosphorylatable (S16A) mutants of HSPB6 were generated using the vector coding for HSPB6 wild-type as template and the QuickChange II Site-Directed Mutagenesis Kit (Agilent Technologies).

**Generation of an HSPB6 phosphorylation mimetic**

Serine 16 of HSPB6 protein was mutated into a cysteine residue (S16C), followed by chemical conversion into a dehydroalanine (Dha) residue. 200 µM of the HSPB6 S16C protein (solubilized in 20 mM phosphate buffer, pH 7.4, was incubated on a shaker (500 rpm) with 5 molar equivalents of methyl 2,5-dibromopentanoate 20 (Merck) for 48 h at 37 °C, obtaining the intermediate product HSPB6-S16Dha. Excess methyl 2,5-dibromopentanoate was removed from HSPB6-S16Dha with 7k MWCO Zeba (Thermo Fisher) spin desalting columns. The conversion of the cysteine residue in position 16 to Dha of HSPB6-S16Dha was verified via LC-MS. Next, to add the phosphate group, 100 µL aliquots of 50 µM HSPB6-S16Dha in 20 nM sodium phosphate buffer, pH 7.4, were reacted batchwise (5 min intervals) with 30,000 molar equivalents of sodium thiophosphate (pH 8.0, 690 mg/mL suspension, 5x5000 equivalents), for 24 h at 37 °C and shaking at 500 rpm. Excess sodium thiophosphate was removed via 7k MWCO Zeba (ThermoFisher) spin desalting columns and reaction was verified via LC-MS.

**Far-UV circular dichroism (CD) spectroscopy**

CD samples were prepared by incubating 25 µM of HSPBs in 20 mM phosphate buffer, pH 6.5 or 5.5. Far-UV CD spectra were recorded on a JASCO J-810 spectrophotometer (JASCO UK, Ltd) equipped with a Peltier thermally controlled cuvette holder at 30 °C (PIKE Technologies). Quartz cuvettes with path lengths of 1 mm were used and CD spectra were obtained by averaging three individual spectra recorded between wavelengths of 250 and 200 nm, with a bandwidth of 1 nm, a data pitch of 0.2 nm, a scanning speed of 50 nm/min, and a response time of 1 sec. For each protein sample, the CD signal of the buffer used to solubilize the protein, or the signal of DMPS alone, was recorded and subtracted from the CD signal of the protein. The CD data was normalized in molar ellipticity per residue as per [q]res(deg cm2 dmol-1) = [q(mdeg) • mol weight > (g/mol)] / [(10 • number of res.• optical path(cm) • C (mg/cm3)].

**Preparation of α-syn seed fibrils**

α-syn seed fibrils were produced as described previously [69]. 500 µL samples of α-syn at concentrations from 500 - 800 µM were incubated in 20 mM phosphate buffer, pH 6.5, for 48 h at about 40 °C and stirred at 1,500 rpm with a Teflon bar on an RCT Basic Heat Plate (IKA, Staufen, Germany). Fibrils were diluted to a monomer equivalent concentration of 200 µM, divided into aliquots, flash frozen in liquid N2 and stored at -80 °C. For experiments at pH 6.5 the 200 µM fibril stock was sonicated for 30-60 sec using a probe sonicator (Bandelin, Sonopuls HD 2070, Berlin, Germany) set at 10% maximum power and 50% cycle. For experiments at low pH with low seed, the 200 µM stock was diluted to 10 µM in water, sonicated 3 times for 5 sec using 10% maximum

power and 50% cycles.

**Measurements of aggregation kinetics (ThT assay)**

20 µM α-syn was incubated in the presence or absence of HSPBs and with 50 µM thioflavin T (ThT, Merck) and either preformed fibrils or DMPS vesicles at 37 °C or 30 °C, respectively [11]. The change in the ThT fluorescence signal was monitored using a Fluostar Optima or Polarstar Omega fluorescence plate reader (BMG Labtech, Aylesbury, UK) in bottom reading mode under quiescent conditions. The concentrations of monomeric and fibrillar states of the protein were determined at the end of each aggregation experiment as previously described[11].

**Labeling α-syn and HSPB6**

The N122C cysteine variant of α-syn [80] and wild-type HSPB6 were buffer exchanged into phosphate buffer, pH 7.4, by use of P10 desalting columns packed with Sephadex G25 matrix (GE Healthcare). The protein was incubated overnight at 4 °C on a rolling system with an excess of Alexa-488 with maleimide moieties (Thermofisher Scientific) at a molar ratio protein-to-dye of 1:1.5. To separate the labelled protein from the free dye, the labelling mixture was loaded onto a Superdex 200 16/600 (GE Healthcare) and eluted in 10 mM phosphate buffer, pH 7.4, at 20 °C. The concentration of the labelled protein was estimated by the absorbance of the fluorophores, assuming a 1:1 labelling stoichiometry (Alexa-488: 72000 $M^{-1}$ $cm^{-1}$ at 495 nm).

**Binding affinity assay**

To determine the binding of α-syn or HSPB6 to lipid vesicles, we measured the change in the effective hydrodynamic radius (Rh) of the protein with increasing SUVs concentration. Measurements were done using 1 µM α-syn-S9C-AL488 and 4 µM α-syn or 1 µM HSPB6-AL488 and 4 µM HSPB6 at 25 °C in 20 mM phosphate buffer pH 7.4. Progressive dilutions of SUV stock solution were prepared in 20 mM phosphate buffer pH 7.4. Samples were prepared with 3.5 µL of labelled protein, together with a varying concentration of the SUV of interest, and 3.5 µL of 20 mM phosphate buffer pH 7.4 in a 24-sample chip-plate. All the measurements were performed on a Fluidity One-W instrument (Fluidic Analytics, Cambridge, UK). Next, the change in the fraction of protein bound to lipid vesicles was fitted using:

Fraction bound $= \frac{X - Xmin}{Xmax - Xmin}$;

where *X* = data point at specific lipid concentration (Rh); *Xmin* = Rh of free protein; *Xmax* = Rh of fully bound protein.

**Analysis of the aggregation kinetics: Determination of the lipid-induced aggregation rate**

The change in mass concentration of fibrils, M(t), was fitted using the single-step nucleation model described previously[11]:

$$\mathrm{M(t)} = \frac{\mathrm{K_M k + m(0)^{n+1} k_n b t^2}}{2\left(\mathrm{K_M + m(0)}\right)}$$

where $k_+$ is the elongation rate constant of fibrils from lipid vesicles, $k_n$ is the heterogeneous primary nucleation rate constant, n is the reaction order of the heterogeneous primary nucleation reaction relative to the free monomer, m, b is the total mass concentration of the protein bound to the lipid at 100% coverage ($\mathrm{b} = \frac{[\mathrm{DMPS}]}{\mathrm{L}}$, with L the stoichiometry) and $K_M$ is the Michaelis constant (fixed at 125 µM, as determined previously[7]. This global analysis yields $k_n k_+$ and n, for each variant. We then estimated the rate of aggregation of each variant on lipid vesicles, using AmyloFit[101] to fit the kinetics to the model described above.

**QUANTIFICATION AND STATISTICAL ANALYSIS**

All statistical analysis were performed using one-way analysis of variance (ANOVA), followed by Bonferroni–Holm *post hoc* test using Daniel's XL Toolbox or GraphPad Prism8 software. The data are shown as mean values of 3 independent experiments and error bars represent mean ± sem. Statistical significance was set at $P < 0.05$.

**References**


1. Yang, Y., Shi, Y., Schweighauser, M., Zhang, X., Kotecha, A., Murzin, A.G., Garringer, H.J., Cullinane, P.W., Saito, Y., Foroud, T., et al. (2022). Structures of alpha-synuclein filaments from human brains with Lewy pathology. Nature *610*, 791-795. 10.1038/s41586-022-05319-3.
2. Sulzer, D., and Edwards, R.H. (2019). The physiological role of alpha-synuclein and its relationship to Parkinson's Disease. J Neurochem *150*, 475-486. 10.1111/jnc.14810.
3. Sharma, M., and Burre, J. (2023). alpha-Synuclein in synaptic function and dysfunction. Trends Neurosci *46*, 153-166. 10.1016/j.tins.2022.11.007.
4. Lautenschlager, J., Kaminski, C.F., and Kaminski Schierle, G.S. (2017). alpha-Synuclein - Regulator of Exocytosis, Endocytosis, or Both? Trends Cell Biol *27*, 468-479. 10.1016/j.tcb.2017.02.002.
5. Eliezer, D., Kutluay, E., Bussell, R., Jr., and Browne, G. (2001). Conformational properties of alpha-synuclein in its free and lipid-associated states. J Mol Biol *307*, 1061-1073. 10.1006/jmbi.2001.4538.
6. Galvagnion, C., Brown, J.W., Ouberai, M.M., Flagmeier, P., Vendruscolo, M., Buell, A.K., Sparr, E., and Dobson, C.M. (2016). Chemical properties of lipids strongly affect the kinetics of the membrane-induced aggregation of alpha-synuclein. Proc Natl Acad Sci U S A *113*, 7065-7070. 10.1073/pnas.1601899113.
7. Galvagnion, C., Buell, A.K., Meisl, G., Michaels, T.C., Vendruscolo, M., Knowles, T.P., and Dobson, C.M. (2015). Lipid vesicles trigger alpha-synuclein aggregation by stimulating primary nucleation. Nat Chem Biol *11*, 229-234. 10.1038/nchembio.1750.
8. Killinger, B.A., Melki, R., Brundin, P., and Kordower, J.H. (2019). Endogenous alpha-synuclein monomers, oligomers and resulting pathology: let's talk about the lipids in the room. NPJ Parkinsons Dis *5*, 23. 10.1038/s41531-019-0095-3.
9. Calabresi, P., Mechelli, A., Natale, G., Volpicelli-Daley, L., Di Lazzaro, G., and Ghiglieri, V. (2023). Alpha-synuclein in Parkinson's disease and other synucleinopathies: from overt neurodegeneration back to early synaptic dysfunction. Cell Death Dis *14*, 176. 10.1038/s41419-023-05672-9.
10. Lashuel, H.A. (2021). Rethinking protein aggregation and drug discovery in neurodegenerative diseases: Why we need to embrace complexity? Curr Opin Chem Biol *64*, 67-75. 10.1016/j.cbpa.2021.05.006.
11. Flagmeier, P., Meisl, G., Vendruscolo, M., Knowles, T.P., Dobson, C.M., Buell, A.K., and Galvagnion, C. (2016). Mutations associated with familial Parkinson's disease alter the initiation and amplification steps of alpha-synuclein aggregation. Proc Natl Acad Sci U S A *113*, 10328-10333. 10.1073/pnas.1604645113.
12. Tsuang, D., Leverenz, J.B., Lopez, O.L., Hamilton, R.L., Bennett, D.A., Schneider, J.A., Buchman, A.S., Larson, E.B., Crane, P.K., Kaye, J.A., et al. (2012). GBA mutations increase risk for Lewy body disease with and without Alzheimer disease pathology. Neurology *79*, 1944-1950. 10.1212/WNL.0b013e3182735e9a.
13. Alecu, I., and Bennett, S.A.L. (2019). Dysregulated Lipid Metabolism and Its Role in alpha-Synucleinopathy in Parkinson's Disease. Front Neurosci *13*, 328. 10.3389/fnins.2019.00328.
14. Fanning, S., Selkoe, D., and Dettmer, U. (2020). Parkinson's disease: proteinopathy or lipidopathy? NPJ Parkinsons Dis *6*, 3. 10.1038/s41531-019-0103-7.
15. Cohen, S.I., Vendruscolo, M., Dobson, C.M., and Knowles, T.P. (2012). From macroscopic measurements to microscopic mechanisms of protein aggregation. J Mol Biol *421*, 160-171. 10.1016/j.jmb.2012.02.031.
16. Ray, S., Singh, N., Kumar, R., Patel, K., Pandey, S., Datta, D., Mahato, J., Panigrahi, R., Navalkar, A., Mehra, S., et al. (2020). alpha-Synuclein aggregation nucleates through liquid-liquid phase separation. Nat Chem *12*, 705-716. 10.1038/s41557-020-0465-9.
17. Hardenberg, M., Horvath, A., Ambrus, V., Fuxreiter, M., and Vendruscolo, M. (2020). Widespread occurrence of the droplet state of proteins in the human proteome. Proc Natl Acad Sci U S A *117*, 33254-33262. 10.1073/pnas.2007670117.
18. Hardenberg, M.C., Sinnige, T., Casford, S., Dada, S.T., Poudel, C., Robinson, E.A., Fuxreiter, M., Kaminksi, C.F., Kaminski Schierle, G.S., Nollen, E.A.A., et al. (2021). Observation of an alpha-synuclein liquid droplet state and its maturation into Lewy body-like assemblies. J Mol Cell Biol *13*, 282-294. 10.1093/jmcb/mjaa075.

19. Dada, S.T., Hardenberg, M.C., Toprakcioglu, Z., Mrugalla, L.K., Cali, M.P., McKeon, M.O., Klimont, E., Michaels, T.C.T., Knowles, T.P.J., and Vendruscolo, M. (2023). Spontaneous nucleation and fast aggregate-dependent proliferation of alpha-synuclein aggregates within liquid condensates at neutral pH. Proc Natl Acad Sci U S A *120*, e2208792120. 10.1073/pnas.2208792120.
20. Arosio, P., Michaels, T.C., Linse, S., Mansson, C., Emanuelsson, C., Presto, J., Johansson, J., Vendruscolo, M., Dobson, C.M., and Knowles, T.P. (2016). Kinetic analysis reveals the diversity of microscopic mechanisms through which molecular chaperones suppress amyloid formation. Nat Commun *7*, 10948. 10.1038/ncomms10948.
21. Boczek, E.E., Fursch, J., Niedermeier, M.L., Jawerth, L., Jahnel, M., Ruer-Gruss, M., Kammer, K.M., Heid, P., Mediani, L., Wang, J., et al. (2021). HspB8 prevents aberrant phase transitions of FUS by chaperoning its folded RNA-binding domain. Elife *10*. 10.7554/eLife.69377.
22. Tao, J., Berthet, A., Citron, Y.R., Tsiolaki, P.L., Stanley, R., Gestwicki, J.E., Agard, D.A., and McConlogue, L. (2021). Hsp70 chaperone blocks alpha-synuclein oligomer formation via a novel engagement mechanism. J Biol Chem *296*, 100613. 10.1016/j.jbc.2021.100613.
23. Schneider, M.M., Gautam, S., Herling, T.W., Andrzejewska, E., Krainer, G., Miller, A.M., Trinkaus, V.A., Peter, Q.A.E., Ruggeri, F.S., Vendruscolo, M., et al. (2021). The Hsc70 disaggregation machinery removes monomer units directly from alpha-synuclein fibril ends. Nat Commun *12*, 5999. 10.1038/s41467-021-25966-w.
24. Kappe, G., Franck, E., Verschuure, P., Boelens, W.C., Leunissen, J.A., and de Jong, W.W. (2003). The human genome encodes 10 alpha-crystallin-related small heat shock proteins: HspB1-10. Cell Stress Chaperones *8*, 53-61. 10.1379/1466-1268(2003)8<53:thgecs>2.0.co;2.
25. Cox, D., and Ecroyd, H. (2017). The small heat shock proteins alphaB-crystallin (HSPB5) and Hsp27 (HSPB1) inhibit the intracellular aggregation of alpha-synuclein. Cell Stress Chaperones *22*, 589-600. 10.1007/s12192-017-0785-x.
26. Selig, E.E., Zlatic, C.O., Cox, D., Mok, Y.F., Gooley, P.R., Ecroyd, H., and Griffin, M.D.W. (2020). N- and C-terminal regions of alphaB-crystallin and Hsp27 mediate inhibition of amyloid nucleation, fibril binding, and fibril disaggregation. J Biol Chem *295*, 9838-9854. 10.1074/jbc.RA120.012748.
27. Vicente Miranda, H., Chegao, A., Oliveira, M.S., Fernandes Gomes, B., Enguita, F.J., and Outeiro, T.F. (2020). Hsp27 reduces glycation-induced toxicity and aggregation of alpha-synuclein. FASEB J *34*, 6718-6728. 10.1096/fj.201902936R.
28. Bruinsma, I.B., Bruggink, K.A., Kinast, K., Versleijen, A.A., Segers-Nolten, I.M., Subramaniam, V., Kuiperij, H.B., Boelens, W., de Waal, R.M., and Verbeek, M.M. (2011). Inhibition of alpha-synuclein aggregation by small heat shock proteins. Proteins *79*, 2956-2967. 10.1002/prot.23152.
29. Cox, D., Carver, J.A., and Ecroyd, H. (2014). Preventing alpha-synuclein aggregation: the role of the small heat-shock molecular chaperone proteins. Biochim Biophys Acta *1842*, 1830-1843. 10.1016/j.bbadis.2014.06.024.
30. Rekas, A., Adda, C.G., Andrew Aquilina, J., Barnham, K.J., Sunde, M., Galatis, D., Williamson, N.A., Masters, C.L., Anders, R.F., Robinson, C.V., et al. (2004). Interaction of the molecular chaperone alphaB-crystallin with alpha-synuclein: effects on amyloid fibril formation and chaperone activity. J Mol Biol *340*, 1167-1183. 10.1016/j.jmb.2004.05.054.
31. Renkawek, K., Stege, G.J., and Bosman, G.J. (1999). Dementia, gliosis and expression of the small heat shock proteins hsp27 and alpha B-crystallin in Parkinson's disease. Neuroreport *10*, 2273-2276. 10.1097/00001756-199908020-00009.
32. Seidel, K., Vinet, J., Dunnen, W.F., Brunt, E.R., Meister, M., Boncoraglio, A., Zijlstra, M.P., Boddeke, H.W., Rub, U., Kampinga, H.H., and Carra, S. (2012). The HSPB8-BAG3 chaperone complex is upregulated in astrocytes in the human brain affected by protein aggregation diseases. Neuropathol Appl Neurobiol *38*, 39-53. 10.1111/j.1365-2990.2011.01198.x.
33. Chowdary, T.K., Raman, B., Ramakrishna, T., and Rao Ch, M. (2007). Interaction of mammalian Hsp22 with lipid membranes. Biochem J *401*, 437-445. 10.1042/BJ20061046.

34. Lopez, V., Cauvi, D.M., Arispe, N., and De Maio, A. (2016). Bacterial Hsp70 (DnaK) and mammalian Hsp70 interact differently with lipid membranes. Cell Stress Chaperones *21*, 609-616. 10.1007/s12192-016-0685-5.
35. De Maio, A., Cauvi, D.M., Capone, R., Bello, I., Egberts, W.V., Arispe, N., and Boelens, W. (2019). The small heat shock proteins, HSPB1 and HSPB5, interact differently with lipid membranes. Cell Stress Chaperones *24*, 947-956. 10.1007/s12192-019-01021-y.
36. Auluck, P.K., Caraveo, G., and Lindquist, S. (2010). alpha-Synuclein: membrane interactions and toxicity in Parkinson's disease. Annu Rev Cell Dev Biol *26*, 211-233. 10.1146/annurev.cellbio.042308.113313.
37. Dores-Silva, P.R., Cauvi, D.M., Coto, A.L.S., Silva, N.S.M., Borges, J.C., and De Maio, A. (2021). Human heat shock cognate protein (HSC70/HSPA8) interacts with negatively charged phospholipids by a different mechanism than other HSP70s and brings HSP90 into membranes. Cell Stress Chaperones *26*, 671-684. 10.1007/s12192-021-01210-8.
38. Balogi, Z., Multhoff, G., Jensen, T.K., Lloyd-Evans, E., Yamashima, T., Jaattela, M., Harwood, J.L., and Vigh, L. (2019). Hsp70 interactions with membrane lipids regulate cellular functions in health and disease. Prog Lipid Res *74*, 18-30. 10.1016/j.plipres.2019.01.004.
39. Tsvetkova, N.M., Horvath, I., Torok, Z., Wolkers, W.F., Balogi, Z., Shigapova, N., Crowe, L.M., Tablin, F., Vierling, E., Crowe, J.H., and Vigh, L. (2002). Small heat-shock proteins regulate membrane lipid polymorphism. Proc Natl Acad Sci U S A *99*, 13504-13509. 10.1073/pnas.192468399.
40. D'Anneo, A., Bavisotto, C.C., Gammazza, A.M., Paladino, L., Carlisi, D., Cappello, F., de Macario, E.C., Macario, A.J.L., and Lauricella, M. (2020). Lipid chaperones and associated diseases: a group of chaperonopathies defining a new nosological entity with implications for medical research and practice. Cell Stress Chaperones *25*, 805-820. 10.1007/s12192-020-01153-6.
41. Sciacca, M.F., Lolicato, F., Tempra, C., Scollo, F., Sahoo, B.R., Watson, M.D., Garcia-Vinuales, S., Milardi, D., Raudino, A., Lee, J.C., et al. (2020). Lipid-Chaperone Hypothesis: A Common Molecular Mechanism of Membrane Disruption by Intrinsically Disordered Proteins. ACS Chem Neurosci *11*, 4336-4350. 10.1021/acschemneuro.0c00588.
42. Carra, S., Alberti, S., Benesch, J.L.P., Boelens, W., Buchner, J., Carver, J.A., Cecconi, C., Ecroyd, H., Gusev, N., Hightower, L.E., et al. (2019). Small heat shock proteins: multifaceted proteins with important implications for life. Cell Stress Chaperones *24*, 295-308. 10.1007/s12192-019-00979-z.
43. Sudnitsyna, M.V., Mymrikov, E.V., Seit-Nebi, A.S., and Gusev, N.B. (2012). The role of intrinsically disordered regions in the structure and functioning of small heat shock proteins. Curr Protein Pept Sci *13*, 76-85. 10.2174/138920312799277875.
44. Boelens, W.C. (2020). Structural aspects of the human small heat shock proteins related to their functional activities. Cell Stress Chaperones *25*, 581-591. 10.1007/s12192-020-01093-1.
45. Weeks, S.D., Baranova, E.V., Heirbaut, M., Beelen, S., Shkumatov, A.V., Gusev, N.B., and Strelkov, S.V. (2014). Molecular structure and dynamics of the dimeric human small heat shock protein HSPB6. J Struct Biol *185*, 342-354. 10.1016/j.jsb.2013.12.009.
46. den Engelsman, J., Boros, S., Dankers, P.Y., Kamps, B., Vree Egberts, W.T., Bode, C.S., Lane, L.A., Aquilina, J.A., Benesch, J.L., Robinson, C.V., et al. (2009). The small heat-shock proteins HSPB2 and HSPB3 form well-defined heterooligomers in a unique 3 to 1 subunit ratio. J Mol Biol *393*, 1022-1032. 10.1016/j.jmb.2009.08.052.
47. Alderson, T.R., Ying, J., Bax, A., Benesch, J.L.P., and Baldwin, A.J. (2020). Conditional Disorder in Small Heat-shock Proteins. J Mol Biol *432*, 3033-3049. 10.1016/j.jmb.2020.02.003.
48. Janowska, M.K., Baughman, H.E.R., Woods, C.N., and Klevit, R.E. (2019). Mechanisms of Small Heat Shock Proteins. Cold Spring Harb Perspect Biol *11*. 10.1101/cshperspect.a034025.
49. Bendifallah, M., Redeker, V., Monsellier, E., Bousset, L., Bellande, T., and Melki, R. (2020). Interaction of the chaperones alpha B-crystallin and CHIP with fibrillar alpha-synuclein: Effects on internalization by cells and identification of interacting interfaces. Biochem Biophys Res Commun *527*, 760-769. 10.1016/j.bbrc.2020.04.091.

50. Cox, D., Whiten, D.R., Brown, J.W.P., Horrocks, M.H., San Gil, R., Dobson, C.M., Klenerman, D., van Oijen, A.M., and Ecroyd, H. (2018). The small heat shock protein Hsp27 binds alpha-synuclein fibrils, preventing elongation and cytotoxicity. J Biol Chem *293*, 4486-4497. 10.1074/jbc.M117.813865.
51. Jia, C., Ma, X., Liu, Z., Gu, J., Zhang, X., Li, D., and Zhang, S. (2019). Different Heat Shock Proteins Bind alpha-Synuclein With Distinct Mechanisms and Synergistically Prevent Its Amyloid Aggregation. Front Neurosci *13*, 1124. 10.3389/fnins.2019.01124.
52. Lu, S.Z., Guo, Y.S., Liang, P.Z., Zhang, S.Z., Yin, S., Yin, Y.Q., Wang, X.M., Ding, F., Gu, X.S., and Zhou, J.W. (2019). Suppression of astrocytic autophagy by alphaB-crystallin contributes to alpha-synuclein inclusion formation. Transl Neurodegener *8*, 3. 10.1186/s40035-018-0143-7.
53. Outeiro, T.F., Klucken, J., Strathearn, K.E., Liu, F., Nguyen, P., Rochet, J.C., Hyman, B.T., and McLean, P.J. (2006). Small heat shock proteins protect against alpha-synuclein-induced toxicity and aggregation. Biochem Biophys Res Commun *351*, 631-638. 10.1016/j.bbrc.2006.10.085.
54. Waudby, C.A., Knowles, T.P., Devlin, G.L., Skepper, J.N., Ecroyd, H., Carver, J.A., Welland, M.E., Christodoulou, J., Dobson, C.M., and Meehan, S. (2010). The interaction of alphaB-crystallin with mature alpha-synuclein amyloid fibrils inhibits their elongation. Biophys J *98*, 843-851. 10.1016/j.bpj.2009.10.056.
55. Perni, M., Flagmeier, P., Limbocker, R., Cascella, R., Aprile, F.A., Galvagnion, C., Heller, G.T., Meisl, G., Chen, S.W., Kumita, J.R., et al. (2018). Multistep Inhibition of alpha-Synuclein Aggregation and Toxicity in Vitro and in Vivo by Trodusquemine. ACS Chem Biol *13*, 2308-2319. 10.1021/acschembio.8b00466.
56. Buell, A.K., Dobson, C.M., and Knowles, T.P. (2014). The physical chemistry of the amyloid phenomenon: thermodynamics and kinetics of filamentous protein aggregation. Essays Biochem *56*, 11-39. 10.1042/bse0560011.
57. Sinning, A., and Hubner, C.A. (2013). Minireview: pH and synaptic transmission. FEBS Lett *587*, 1923-1928. 10.1016/j.febslet.2013.04.045.
58. Fusco, G., Chen, S.W., Williamson, P.T.F., Cascella, R., Perni, M., Jarvis, J.A., Cecchi, C., Vendruscolo, M., Chiti, F., Cremades, N., et al. (2017). Structural basis of membrane disruption and cellular toxicity by alpha-synuclein oligomers. Science *358*, 1440-1443. 10.1126/science.aan6160.
59. Demchenko, A.P., Mely, Y., Duportail, G., and Klymchenko, A.S. (2009). Monitoring biophysical properties of lipid membranes by environment-sensitive fluorescent probes. Biophys J *96*, 3461-3470. 10.1016/j.bpj.2009.02.012.
60. Kato, K., Goto, S., Inaguma, Y., Hasegawa, K., Morishita, R., and Asano, T. (1994). Purification and characterization of a 20-kDa protein that is highly homologous to alpha B crystallin. J Biol Chem *269*, 15302-15309.
61. Edwards, H.V., Scott, J.D., and Baillie, G.S. (2012). PKA phosphorylation of the small heat-shock protein Hsp20 enhances its cardioprotective effects. Biochem Soc Trans *40*, 210-214. 10.1042/BST20110673.
62. Chernik, I.S., Seit-Nebi, A.S., Marston, S.B., and Gusev, N.B. (2007). Small heat shock protein Hsp20 (HspB6) as a partner of 14-3-3gamma. Mol Cell Biochem *295*, 9-17. 10.1007/s11010-006-9266-8.
63. Dreiza, C.M., Brophy, C.M., Komalavilas, P., Furnish, E.J., Joshi, L., Pallero, M.A., Murphy-Ullrich, J.E., von Rechenberg, M., Ho, Y.S., Richardson, B., et al. (2005). Transducible heat shock protein 20 (HSP20) phosphopeptide alters cytoskeletal dynamics. FASEB J *19*, 261-263. 10.1096/fj.04-2911fje.
64. Underwood, R., Gannon, M., Pathak, A., Kapa, N., Chandra, S., Klop, A., and Yacoubian, T.A. (2021). 14-3-3 mitigates alpha-synuclein aggregation and toxicity in the in vivo preformed fibril model. Acta Neuropathol Commun *9*, 13. 10.1186/s40478-020-01110-5.
65. Jakubec, M., Barias, E., Furse, S., Govasli, M.L., George, V., Turcu, D., Iashchishyn, I.A., Morozova-Roche, L.A., and Halskau, O. (2021). Cholesterol-containing lipid nanodiscs promote an alpha-synuclein binding mode that accelerates oligomerization. FEBS J *288*, 1887-1905. 10.1111/febs.15551.
66. Sluchanko, N.N., Beelen, S., Kulikova, A.A., Weeks, S.D., Antson, A.A., Gusev, N.B., and Strelkov, S.V. (2017). Structural Basis for the Interaction of a Human Small Heat Shock Protein with the 14-3-3 Universal Signaling Regulator. Structure *25*, 305-316. 10.1016/j.str.2016.12.005.

67. Sluchanko, N.N., Sudnitsyna, M.V., Chernik, I.S., Seit-Nebi, A.S., and Gusev, N.B. (2011). Phosphomimicking mutations of human 14-3-3zeta affect its interaction with tau protein and small heat shock protein HspB6. Arch Biochem Biophys *506*, 24-34. 10.1016/j.abb.2010.11.003.
68. Shammas, S.L., Waudby, C.A., Wang, S., Buell, A.K., Knowles, T.P., Ecroyd, H., Welland, M.E., Carver, J.A., Dobson, C.M., and Meehan, S. (2011). Binding of the molecular chaperone alphaB-crystallin to Abeta amyloid fibrils inhibits fibril elongation. Biophys J *101*, 1681-1689. 10.1016/j.bpj.2011.07.056.
69. Buell, A.K., Galvagnion, C., Gaspar, R., Sparr, E., Vendruscolo, M., Knowles, T.P., Linse, S., and Dobson, C.M. (2014). Solution conditions determine the relative importance of nucleation and growth processes in alpha-synuclein aggregation. Proc Natl Acad Sci U S A *111*, 7671-7676. 10.1073/pnas.1315346111.
70. Rajagopal, P., Tse, E., Borst, A.J., Delbecq, S.P., Shi, L., Southworth, D.R., and Klevit, R.E. (2015). A conserved histidine modulates HSPB5 structure to trigger chaperone activity in response to stress-related acidosis. Elife *4*. 10.7554/eLife.07304.
71. Maroteaux, L., Campanelli, J.T., and Scheller, R.H. (1988). Synuclein: a neuron-specific protein localized to the nucleus and presynaptic nerve terminal. J Neurosci *8*, 2804-2815. 10.1523/JNEUROSCI.08-08-02804.1988.
72. Kahle, P.J., Neumann, M., Ozmen, L., Muller, V., Jacobsen, H., Schindzielorz, A., Okochi, M., Leimer, U., van Der Putten, H., Probst, A., et al. (2000). Subcellular localization of wild-type and Parkinson's disease-associated mutant alpha -synuclein in human and transgenic mouse brain. J Neurosci *20*, 6365-6373. 10.1523/JNEUROSCI.20-17-06365.2000.
73. Snead, D., and Eliezer, D. (2014). Alpha-synuclein function and dysfunction on cellular membranes. Exp Neurobiol *23*, 292-313. 10.5607/en.2014.23.4.292.
74. Miraglia, F., Ricci, A., Rota, L., and Colla, E. (2018). Subcellular localization of alpha-synuclein aggregates and their interaction with membranes. Neural Regen Res *13*, 1136-1144. 10.4103/1673-5374.235013.
75. Nakamura, K., Nemani, V.M., Wallender, E.K., Kaehlcke, K., Ott, M., and Edwards, R.H. (2008). Optical reporters for the conformation of alpha-synuclein reveal a specific interaction with mitochondria. J Neurosci *28*, 12305-12317. 10.1523/JNEUROSCI.3088-08.2008.
76. Choi, M.L., Chappard, A., Singh, B.P., Maclachlan, C., Rodrigues, M., Fedotova, E.I., Berezhnov, A.V., De, S., Peddie, C.J., Athauda, D., et al. (2022). Author Correction: Pathological structural conversion of alpha-synuclein at the mitochondria induces neuronal toxicity. Nat Neurosci *25*, 1582. 10.1038/s41593-022-01206-2.
77. Cooper, A.A., Gitler, A.D., Cashikar, A., Haynes, C.M., Hill, K.J., Bhullar, B., Liu, K., Xu, K., Strathearn, K.E., Liu, F., et al. (2006). Alpha-synuclein blocks ER-Golgi traffic and Rab1 rescues neuron loss in Parkinson's models. Science *313*, 324-328. 10.1126/science.1129462.
78. Hipp, M.S., Kasturi, P., and Hartl, F.U. (2019). The proteostasis network and its decline in ageing. Nat Rev Mol Cell Biol *20*, 421-435. 10.1038/s41580-019-0101-y.
79. Gao, X., Carroni, M., Nussbaum-Krammer, C., Mogk, A., Nillegoda, N.B., Szlachcic, A., Guilbride, D.L., Saibil, H.R., Mayer, M.P., and Bukau, B. (2015). Human Hsp70 Disaggregase Reverses Parkinson's-Linked alpha-Synuclein Amyloid Fibrils. Mol Cell *59*, 781-793. 10.1016/j.molcel.2015.07.012.
80. Gaspar, R., Meisl, G., Buell, A.K., Young, L., Kaminski, C.F., Knowles, T.P.J., Sparr, E., and Linse, S. (2017). Secondary nucleation of monomers on fibril surface dominates alpha-synuclein aggregation and provides autocatalytic amyloid amplification. Q Rev Biophys *50*, e6. 10.1017/S0033583516000172.
81. Deryusheva, E., Nemashkalova, E., Galloux, M., Richard, C.A., Eleouet, J.F., Kovacs, D., Van Belle, K., Tompa, P., Uversky, V., and Permyakov, S. (2019). Does Intrinsic Disorder in Proteins Favor Their Interaction with Lipids? Proteomics *19*, e1800098. 10.1002/pmic.201800098.
82. Overduin, M., Wille, H., and Westaway, D. (2021). Multisite interactions of prions with membranes and native nanodiscs. Chem Phys Lipids *236*, 105063. 10.1016/j.chemphyslip.2021.105063.
83. van de Klundert, F.A., Smulders, R.H., Gijsen, M.L., Lindner, R.A., Jaenicke, R., Carver, J.A., and de Jong, W.W. (1998). The mammalian small heat-shock protein Hsp20 forms dimers and is a poor chaperone. Eur J Biochem *258*, 1014-1021. 10.1046/j.1432-1327.1998.2581014.x.

84. Mymrikov, E.V., Daake, M., Richter, B., Haslbeck, M., and Buchner, J. (2017). The Chaperone Activity and Substrate Spectrum of Human Small Heat Shock Proteins. J Biol Chem *292*, 672-684. 10.1074/jbc.M116.760413.
85. Zhou, C., Wang, L., Cheng, W., Lv, J., Guan, X., Guo, T., Wu, J., Zhang, W., Gao, T., Liu, X., et al. (2023). Two distinct trajectories of clinical and neurodegeneration events in Parkinson's disease. NPJ Parkinsons Dis *9*, 111. 10.1038/s41531-023-00556-3.
86. Bartelt-Kirbach, B., and Golenhofen, N. (2014). Reaction of small heat-shock proteins to different kinds of cellular stress in cultured rat hippocampal neurons. Cell Stress Chaperones *19*, 145-153. 10.1007/s12192-013-0452-9.
87. Qi, A.Q., Zhang, Y.H., Qi, Q.D., Liu, Y.H., and Zhu, J.L. (2019). Overexpressed HspB6 Underlines a Novel Inhibitory Role in Kainic Acid-Induced Epileptic Seizure in Rats by Activating the cAMP-PKA Pathway. Cell Mol Neurobiol *39*, 111-122. 10.1007/s10571-018-0637-y.
88. Vendredy, L., Adriaenssens, E., and Timmerman, V. (2020). Small heat shock proteins in neurodegenerative diseases. Cell Stress Chaperones *25*, 679-699. 10.1007/s12192-020-01101-4.
89. Navarro-Zaragoza, J., Cuenca-Bermejo, L., Almela, P., Laorden, M.L., and Herrero, M.T. (2021). Could Small Heat Shock Protein HSP27 Be a First-Line Target for Preventing Protein Aggregation in Parkinson's Disease? Int J Mol Sci *22*. 10.3390/ijms22063038.
90. Melki, R. (2018). Alpha-synuclein and the prion hypothesis in Parkinson's disease. Rev Neurol (Paris) *174*, 644-652. 10.1016/j.neurol.2018.08.002.
91. Masaracchia, C., Hnida, M., Gerhardt, E., Lopes da Fonseca, T., Villar-Pique, A., Branco, T., Stahlberg, M.A., Dean, C., Fernandez, C.O., Milosevic, I., and Outeiro, T.F. (2018). Membrane binding, internalization, and sorting of alpha-synuclein in the cell. Acta Neuropathol Commun *6*, 79. 10.1186/s40478-018-0578-1.
92. Fedosejevs, C.S., and Schneider, M.F. (2022). Sharp, localized phase transitions in single neuronal cells. Proc Natl Acad Sci U S A *119*. 10.1073/pnas.2117521119.
93. De Maio, A., and Hightower, L. (2021). The interaction of heat shock proteins with cellular membranes: a historical perspective. Cell Stress Chaperones *26*, 769-783. 10.1007/s12192-021-01228-y.
94. Csoboz, B., Gombos, I., Kota, Z., Dukic, B., Klement, E., Varga-Zsiros, V., Lipinszki, Z., Pali, T., Vigh, L., and Torok, Z. (2022). The Small Heat Shock Protein, HSPB1, Interacts with and Modulates the Physical Structure of Membranes. Int J Mol Sci *23*. 10.3390/ijms23137317.
95. Crul, T., Csoboz, B., Gombos, I., Marton, A., Peter, M., Balogh, G., Vizler, C., Szente, L., and Vigh, L. (2020). Modulation of Plasma Membrane Composition and Microdomain Organization Impairs Heat Shock Protein Expression in B16-F10 Mouse Melanoma Cells. Cells *9*. 10.3390/cells9040951.
96. Torok, Z., Crul, T., Maresca, B., Schutz, G.J., Viana, F., Dindia, L., Piotto, S., Brameshuber, M., Balogh, G., Peter, M., et al. (2014). Plasma membranes as heat stress sensors: from lipid-controlled molecular switches to therapeutic applications. Biochim Biophys Acta *1838*, 1594-1618. 10.1016/j.bbamem.2013.12.015.
97. Hibshman, J.D., Carra, S., and Goldstein, B. (2023). Tardigrade small heat shock proteins can limit desiccation-induced protein aggregation. Commun Biol *6*, 121. 10.1038/s42003-023-04512-y.
98. Galvagnion, C., Barclay, A., Makasewicz, K., Marlet, F.R., Moulin, M., Devos, J.M., Linse, S., Martel, A., Porcar, L., Sparr, E., et al. (2024). Structural characterisation of alpha-synuclein-membrane interactions and the resulting aggregation using small angle scattering. Phys Chem Chem Phys *26*, 10998-11013. 10.1039/d3cp05928f.
99. Carra, S., Sivilotti, M., Chavez Zobel, A.T., Lambert, H., and Landry, J. (2005). HspB8, a small heat shock protein mutated in human neuromuscular disorders, has in vivo chaperone activity in cultured cells. Hum Mol Genet *14*, 1659-1669. 10.1093/hmg/ddi174.
100. Baumann, K.N., Sneideriene, G., Sanguanini, M., Schneider, M., Rimon, O., Gonzalez Diaz, A., Greer, H., Thacker, D., Linse, S., Knowles, T.P.J., and Vendruscolo, M. (2023). A Kinetic Map of the Influence of

Biomimetic Lipid Model Membranes on Abeta(42) Aggregation. ACS Chem Neurosci *14*, 323-329. 10.1021/acschemneuro.2c00765.

101. Meisl, G., Kirkegaard, J.B., Arosio, P., Michaels, T.C., Vendruscolo, M., Dobson, C.M., Linse, S., and Knowles, T.P. (2016). Molecular mechanisms of protein aggregation from global fitting of kinetic models. Nat Protoc *11*, 252-272. 10.1038/nprot.2016.010.

**Figure 1**

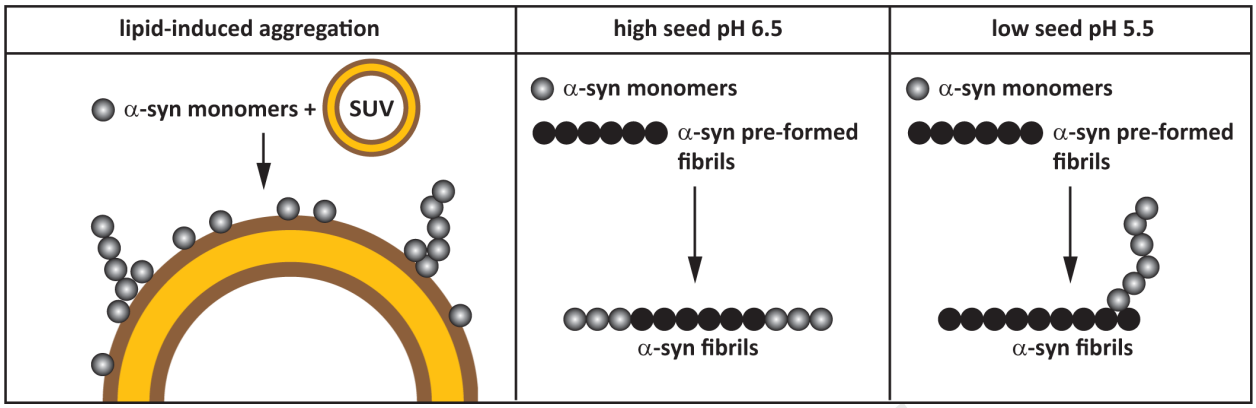

Figure 2

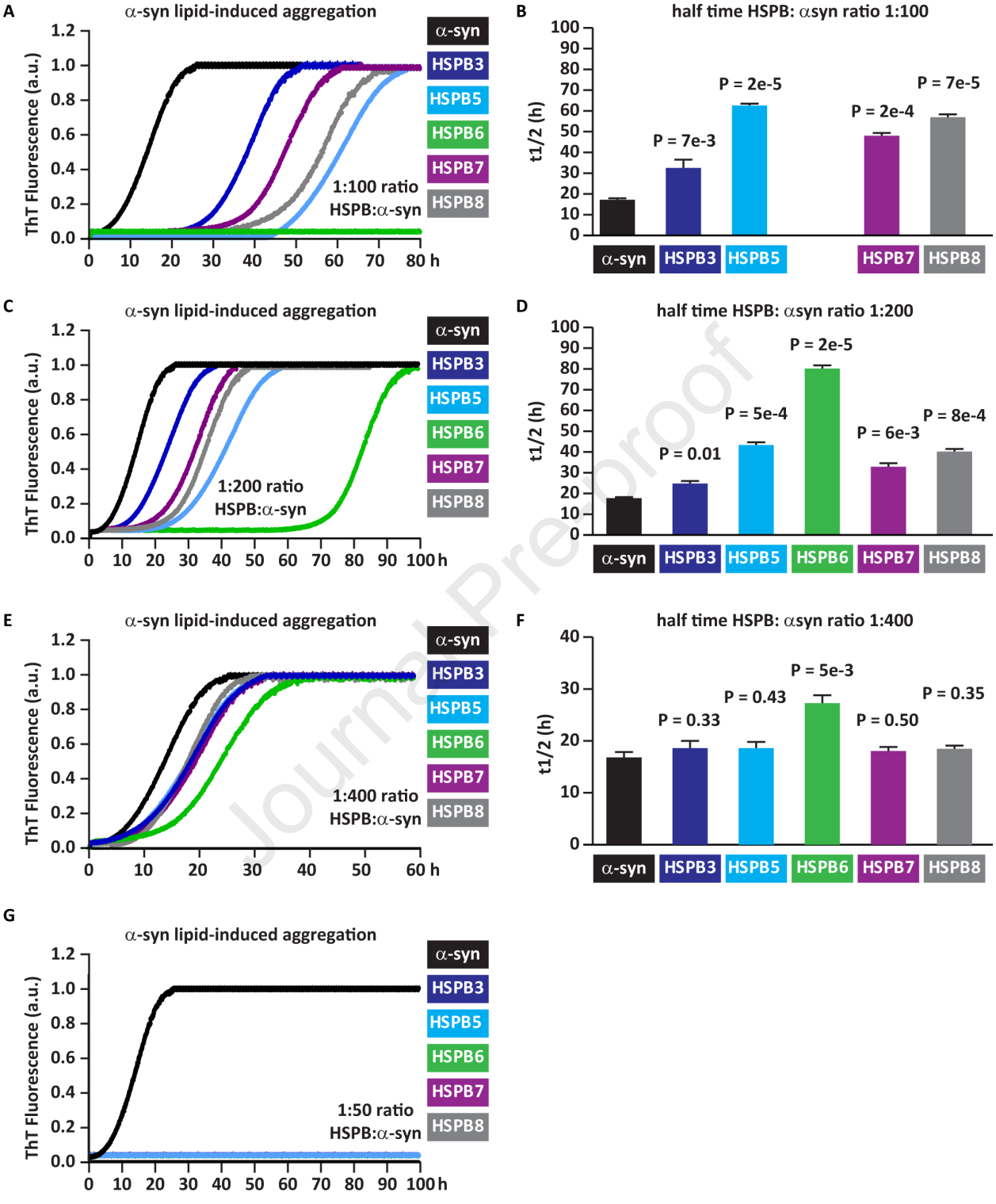

Figure 3

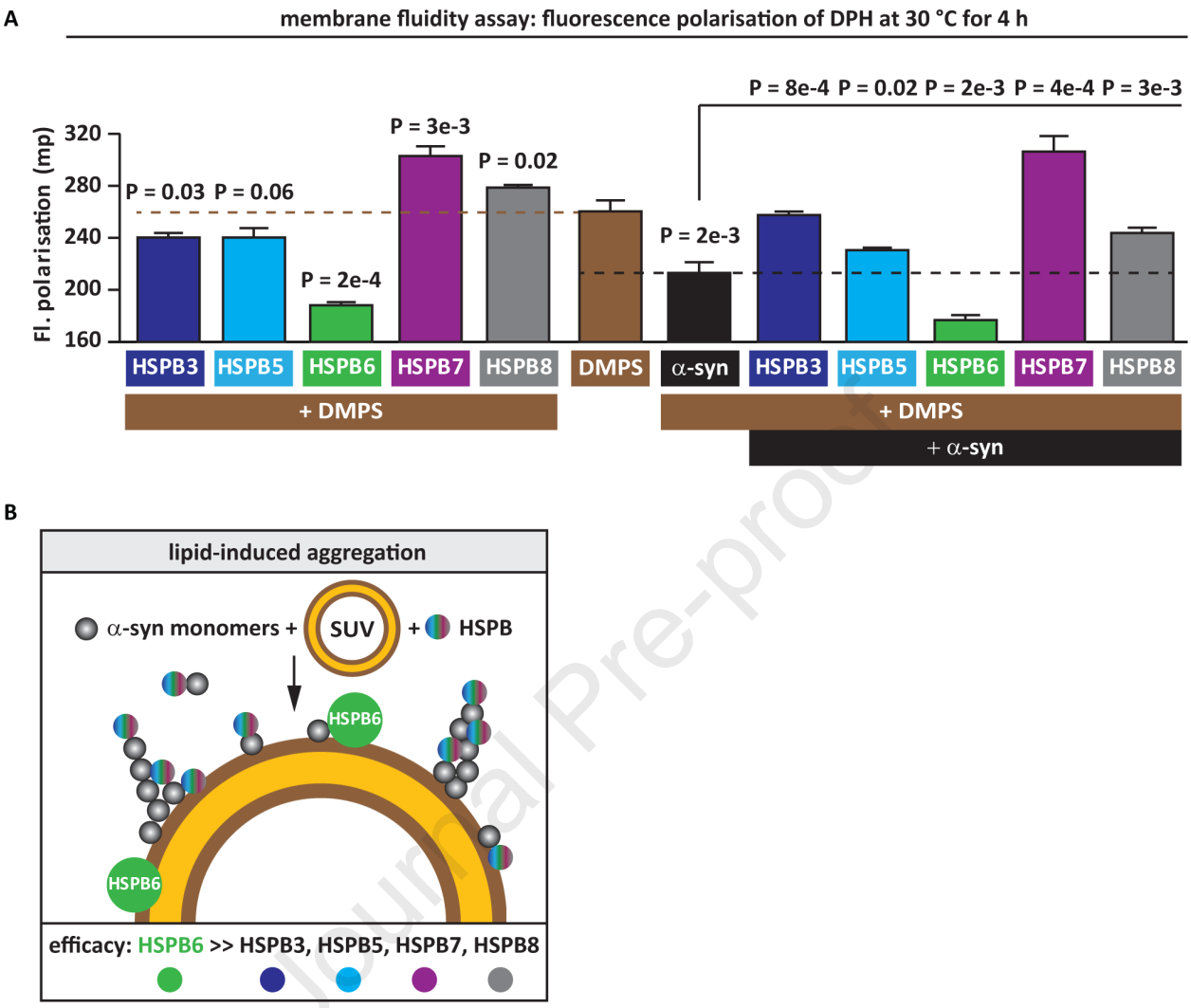

Figure 4

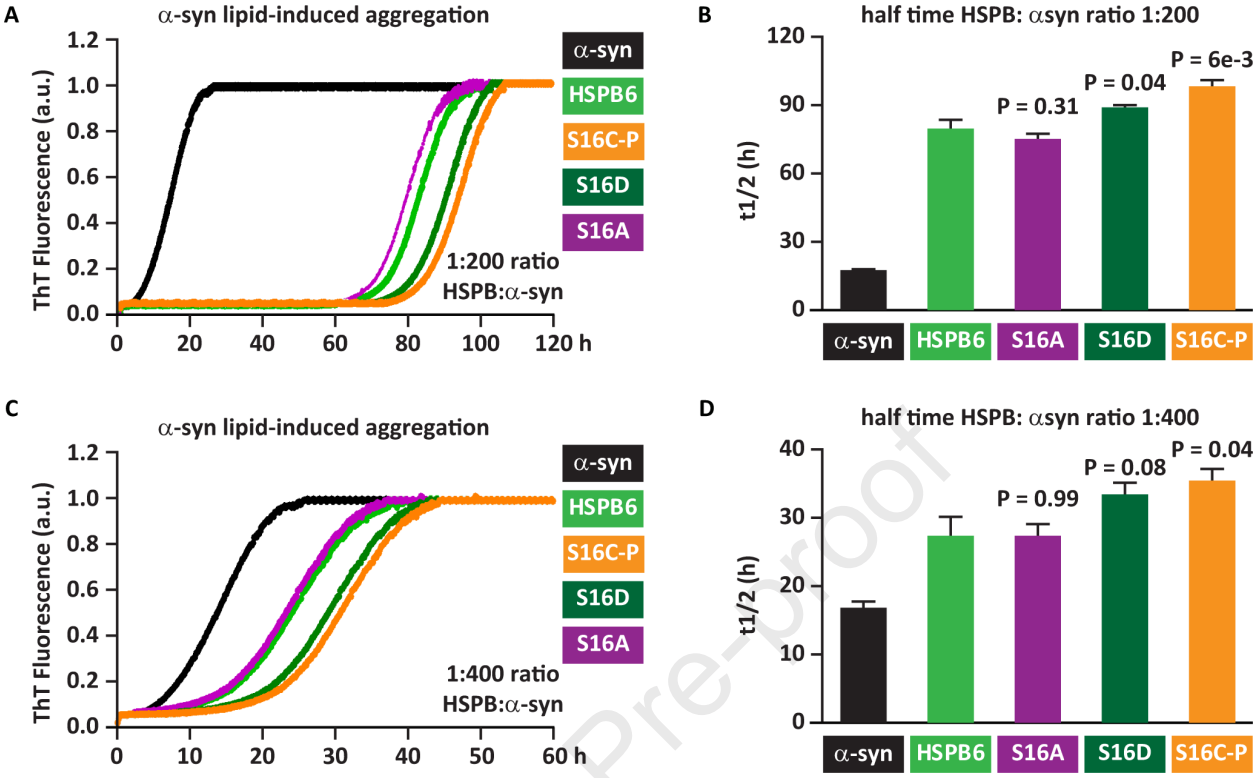

Figure 5

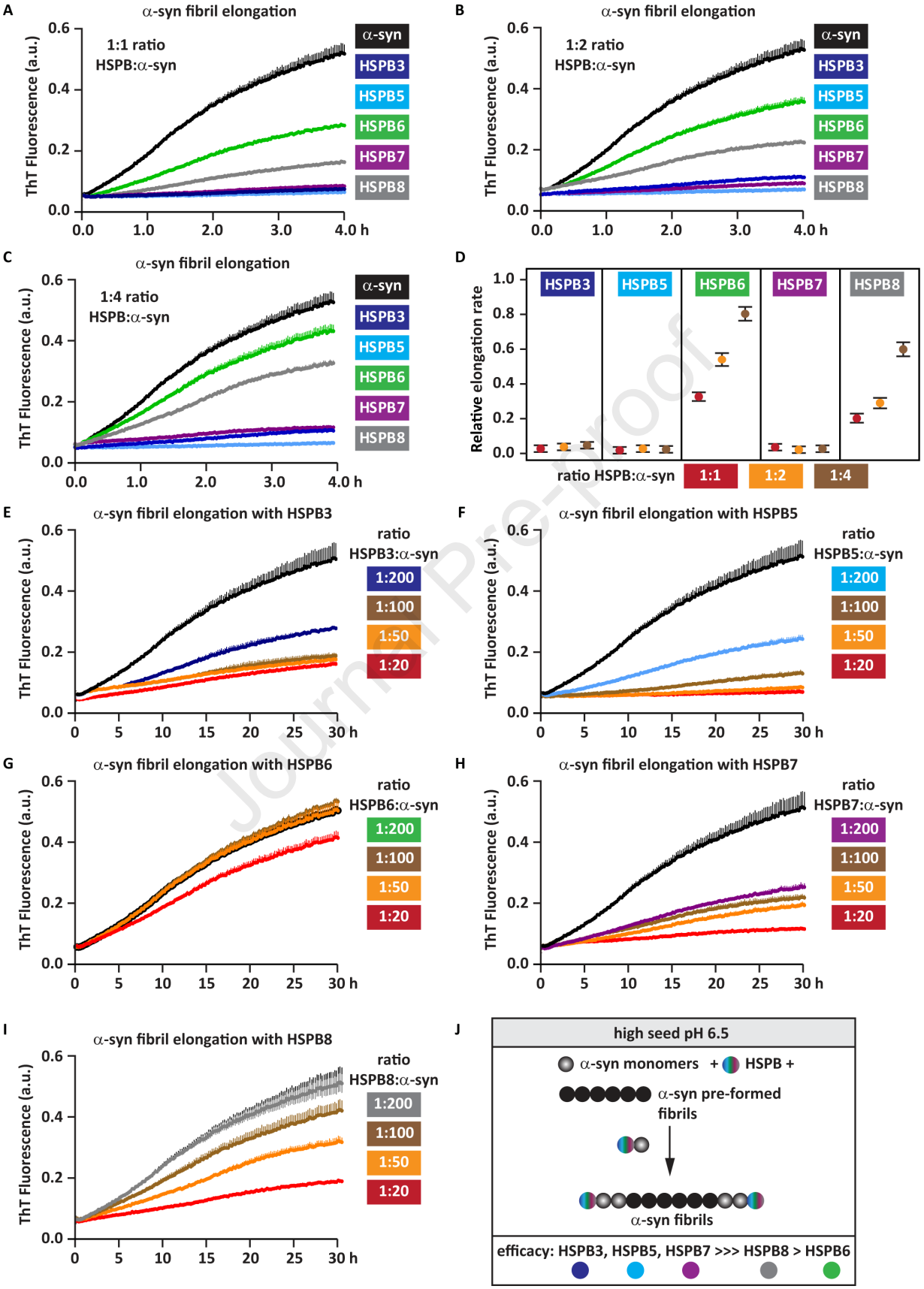
A
α-syn fibril elongation
1:1 ratio
HSPB:α-syn
ThT Fluorescence (a.u.)
α-syn
HSPB3
HSPB5
HSPB6
HSPB7
HSPB8
B
α-syn fibril elongation
1:2 ratio
HSPB:α-syn
C
α-syn fibril elongation
1:4 ratio
HSPB:α-syn
D
Relative elongation rate
ratio HSPB:α-syn
1:1
1:2
1:4
E
α-syn fibril elongation with HSPB3
ratio
HSPB3:α-syn
1:200
1:100
1:50
1:20
F
α-syn fibril elongation with HSPB5
ratio
HSPB5:α-syn
G
α-syn fibril elongation with HSPB6
ratio
HSPB6:α-syn
H
α-syn fibril elongation with HSPB7
ratio
HSPB7:α-syn
I
α-syn fibril elongation with HSPB8
ratio
HSPB8:α-syn
J
high seed pH 6.5
α-syn monomers + HSPB +
α-syn pre-formed fibrils
α-syn fibrils
efficacy: HSPB3, HSPB5, HSPB7 >>> HSPB8 > HSPB6

Figure 6

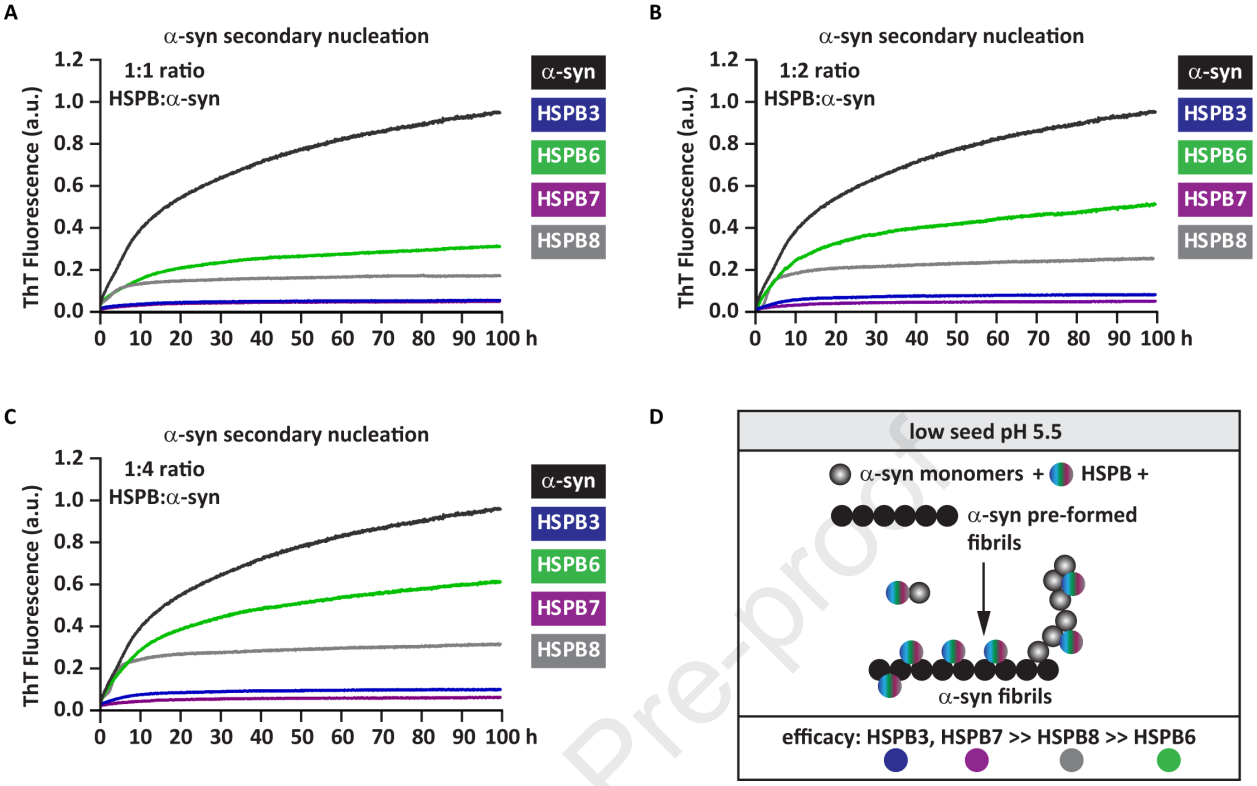

Figure 7

A

| SUV lipid composition | mitochondria | outer PM | inner PM | ER | Golgi |
|---|---|---|---|---|---|
| PC | 35 % | 30 % | 22 % | 52 % | 43 % |
| PE | 41 % | - | 40 % | 26 % | 17 % |
| PI | 24 % | - | - | 9 % | 9 % |
| PS | - | 5 % | 26 % | - | - |
| SM | - | 35 % | - | - | 17 % |
| cholesterol | - | 30 % | 12 % | 13 % | 14 % |

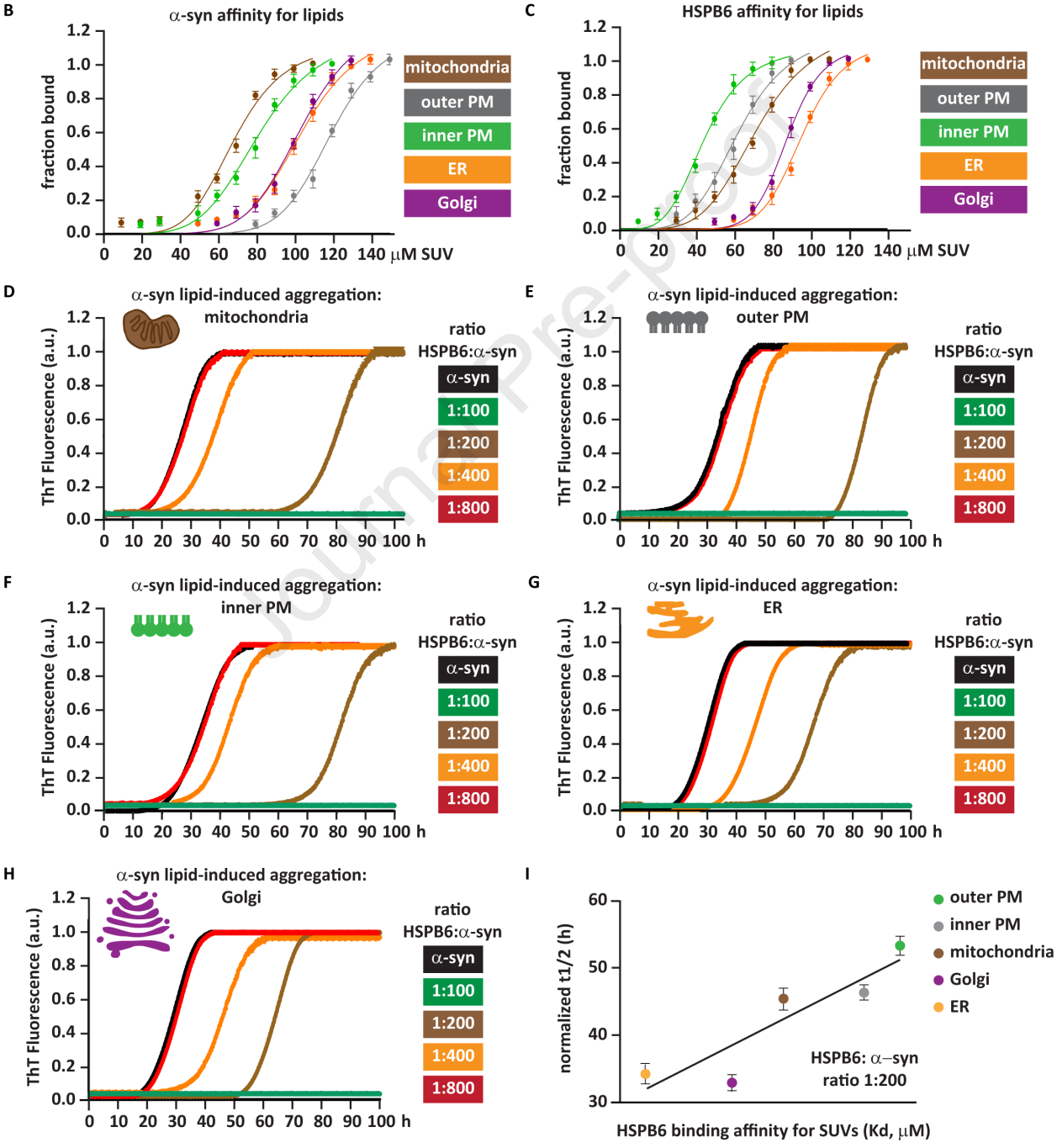

**ISCIENCE-D-24-08168**

**Highlights:**

- α-synuclein aggregation can be modulated by lipids and pH
- HSPBs evolved to inhibit α-synuclein aggregation through multiple mechanisms
- HSPB6 shows a lipid-dependent chaperone activity
- HSPB3, 5, 7 and 8 preferentially act on fibril elongation and secondary nucleation